Article

Cell Stem Cell

NHEJ-Mediated Repair of CRISPR-Cas9-Induced DNA Breaks Efficiently Corrects Mutations in HSPCs from Patients with Fanconi Anemia

Graphical Abstract

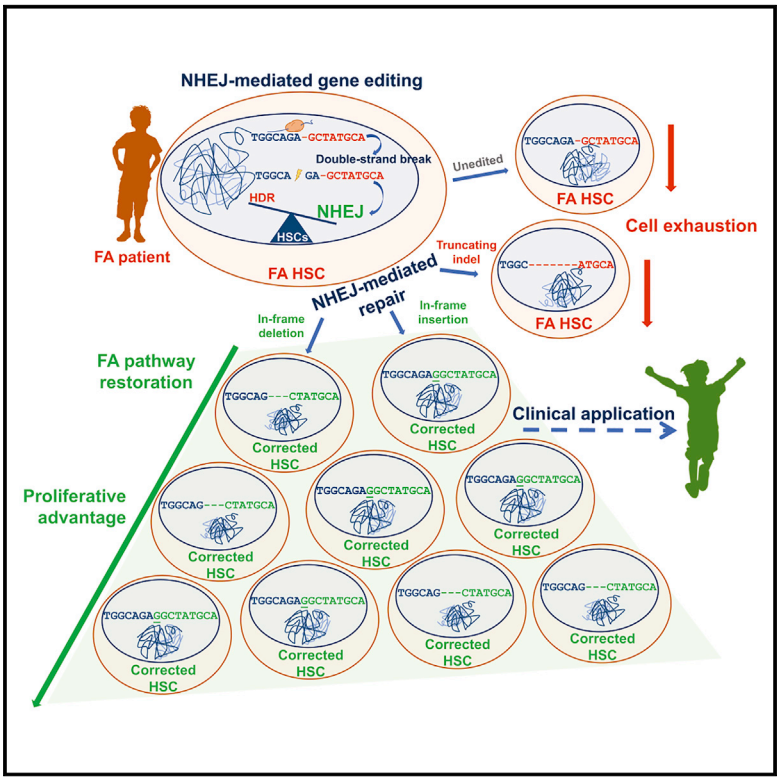

Highlights

- NHEJ-mediated gene editing enables highly efficient editing in human long-term HSCs
- NHEJ-mediated editing restores mutant coding frames across FA complementation groups
- Corrected FA-HSCs have a marked proliferative advantage *in vitro* and *in vivo*

Authors

Francisco José Román-Rodríguez, Laura Ugalde, Lara Álvarez, ..., Jordi Surrallés, Juan Antonio Bueren, Paula Río

Correspondence

paula.rio@ciemat.es

In Brief

NHEJ is an error-prone DSB repair mechanism typically exploited to create gene knockouts. Román-Rodríguez and colleagues show efficient CRISPR-Cas9-mediated repair of mutated Fanconi anemia genes using NHEJ to generate compensatory mutations that correct the phenotype of FA patient HSCs, suggesting a simple and feasible clinical approach for monogenic hematopoietic diseases.

Román-Rodríguez et al., 2019, Cell Stem Cell *25*, 607–621
November 7, 2019
https://doi.org/10.1016/j.stem.2019.08.016

CellPress

Cell Stem Cell
Article

NHEJ-Mediated Repair of CRISPR-Cas9-Induced DNA Breaks Efficiently Corrects Mutations in HSPCs from Patients with Fanconi Anemia

Francisco José Román-Rodríguez,[1,2,3] Laura Ugalde,[1,2,3] Lara Álvarez,[1,2,3] Begoña Díez,[1,2,3] María José Ramírez,[2,4,5] Cristina Risueño,[1,2,3] Marta Cortón,[2,6] Massimo Bogliolo,[2,4,5] Sara Bernal,[2,5] Francesca March,[5] Carmen Ayuso,[2,6] Helmut Hanenberg,[7,8] Julián Sevilla,[9] Sandra Rodríguez-Perales,[10] Raúl Torres-Ruiz,[10,11] Jordi Surrallés,[2,4,5] Juan Antonio Bueren,[1,2,3] and Paula Río[1,2,3,12,*]

[1]Division of Hematopoietic Innovative Therapies, Centro de Investigaciones Energéticas Medioambientales y Tecnológicas (CIEMAT), Madrid 28040, Spain
[2]Centro de Investigación Biomédica en Red de Enfermedades Raras (CIBERER-ISCIII), Madrid 28040, Spain
[3]Advanced Therapies Unit, Instituto de Investigación Sanitaria Fundación Jiménez Díaz (IIS-FJD/UAM), Madrid 28040, Spain
[4]Genome Instability and DNA Repair Syndromes Group, Department of Genetics and Microbiology, Universitat Autònoma de Barcelona (UAB), Barcelona 08193, Spain
[5]Servicio de Genética e Instituto de Investigaciones Biomédicas del Hospital de Sant Pau, Barcelona 08025, Spain
[6]Department of Genetics, Hospital Universitario Instituto de Investigación Sanitaria Fundación Jiménez Díaz (IIS-FJD, UAM), Madrid 28040, Spain
[7]Department of Otorhinolaryngology and Head/Neck Surgery, Heinrich Heine University, Düsseldorf 40225, Germany
[8]Department of Pediatrics III, University Children's Hospital Essen, University of Duisburg-Essen, Essen 45122, Germany
[9]Hospital Universitario Niño Jesús, Madrid 28009, Spain
[10]Molecular Cytogenetics Group, Human Cancer Genetics Program, Centro Nacional de Investigaciones Oncológicas (CNIO), Madrid 28029, Spain
[11]Josep Carreras Leukemia Research Institute and Department of Biomedicine, School of Medicine, University of Barcelona, Barcelona 08036, Spain
[12]Lead Contact
*Correspondence: paula.rio@ciemat.es
https://doi.org/10.1016/j.stem.2019.08.016

SUMMARY

Non-homologous end-joining (NHEJ) is the preferred mechanism used by hematopoietic stem cells (HSCs) to repair double-stranded DNA breaks and is particularly increased in cells deficient in the Fanconi anemia (FA) pathway. Here, we show feasible correction of compromised functional phenotypes in hematopoietic cells from multiple FA complementation groups, including FA-A, FA-C, FA-D1, and FA-D2. NHEJ-mediated repair of targeted CRISPR-Cas9-induced DNA breaks generated compensatory insertions and deletions that restore the coding frame of the mutated gene. NHEJ-mediated editing efficacy was initially verified in FA lymphoblastic cell lines and then in primary FA patient-derived CD34$^+$ cells, which showed marked proliferative advantage and phenotypic correction both *in vitro* and after transplantation. Importantly, and in contrast to homologous directed repair, NHEJ efficiently targeted primitive human HSCs, indicating that NHEJ editing approaches may constitute a sound alternative for editing self-renewing human HSCs and consequently for treatment of FA and other monogenic diseases affecting the hematopoietic system.

INTRODUCTION

Allogenic transplantation of hematopoietic stem and progenitor cells (HSPCs) currently constitutes the only curative treatment for bone marrow failure (BMF) characteristic of Fanconi anemia (FA) patients (Ebens et al., 2017). However, its application is hampered by the limited availability of histocompatibility leukocyte antigen (HLA)-matched donors, risks of graft-versus-host disease, and increased incidence of solid tumors in the long term (Guardiola et al., 2004; Kutler et al., 2003).

Correction of patients' HSPCs by gene therapy is a promising therapeutic alternative to allogeneic transplantation due to the proliferative advantage associated with the correction of mutated FA genes. This phenomenon was first observed in mosaic patients in whom secondary mutations in FA genes restored the function of mutated alleles (Gross et al., 2002; Hamanoue et al., 2006; Mankad et al., 2006). In these patients, compensatory mutations occurring in HSPCs resulted in the expansion of the reverted clones, leading to the correction of FA-patient hematopoiesis (Asur et al., 2018; Gregory et al., 2001; Waisfisz et al., 1999). Somatic mosaicism was thus proposed as a natural gene therapy process, suggesting that the correction of a low number of HSCs could be sufficient to restore the hematopoiesis of FA patients. Using an *ex vivo* lentiviral-mediated gene therapy approach, we have recently demonstrated that corrected CD34$^+$ cells from FA patients also develop *in vivo* proliferative advantage in transplanted immunodeficient mice, mimicking the behavior of reverted FA HSCs (Río et al., 2017).

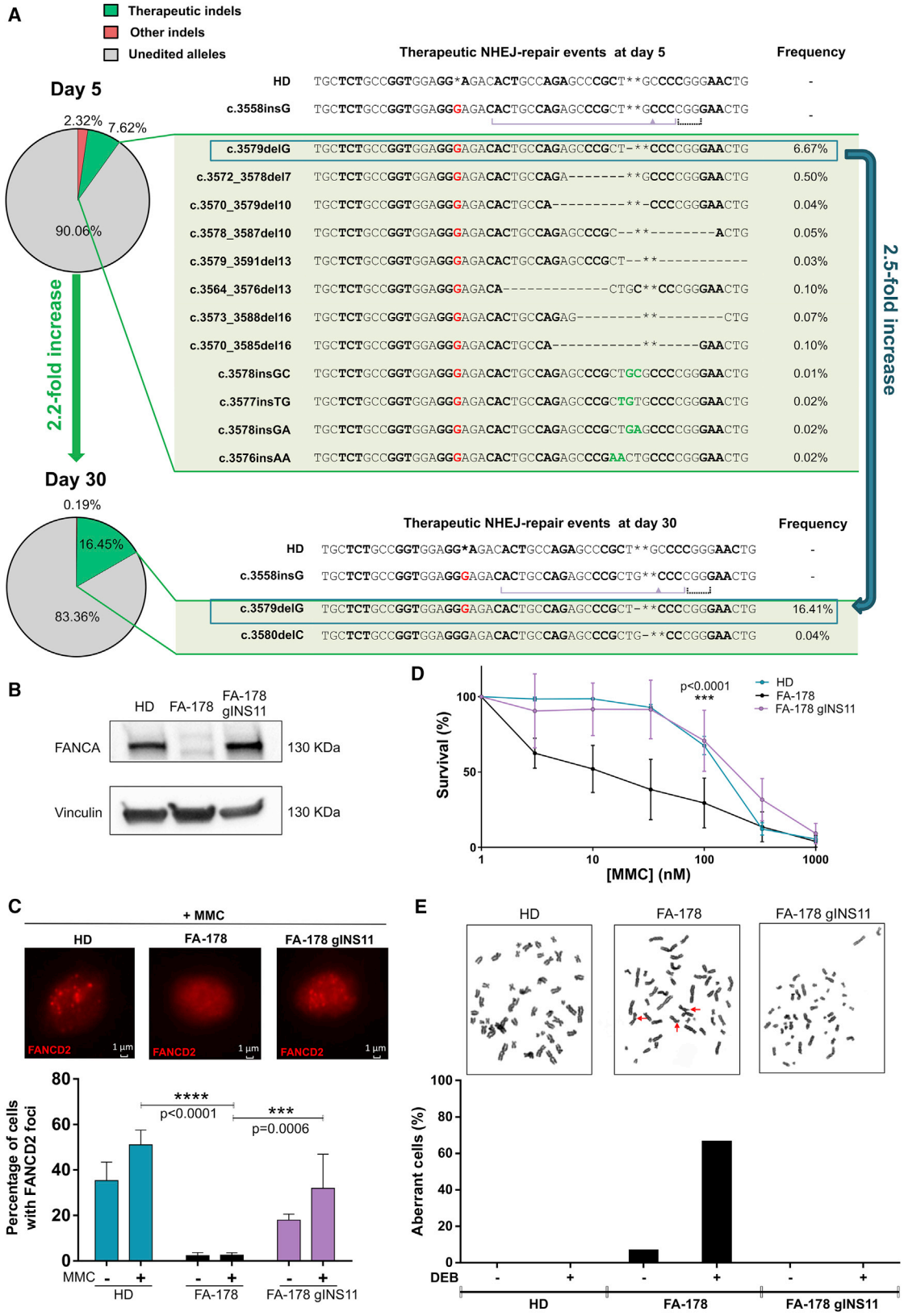

(legend on next page)

Aiming at the precise insertion of therapeutic FA genes, in previous studies we developed homologous recombination (HR)-mediated gene therapy approaches that facilitated the integration of a healthy copy of *FANCA* in the "safe harbor" *AAVS1* locus of FA-A cells, initially in fibroblasts (Río et al., 2014) and thereafter in HSPCs (Diez et al., 2017). Despite advances achieved in HR-mediated gene editing (Bak et al., 2018; De Ravin et al., 2016; Genovese et al., 2014; Schiroli et al., 2017), three pieces of evidence support that non-homologous end-joining (NHEJ)-based editing should constitute a good alternative approach for the editing of FA HSCs. (1) In contrast to NHEJ, HR is less efficient in primitive HSCs as compared to the more differentiated hematopoietic progenitor cells (Lombardo et al., 2007; Wang et al., 2001, 2015; Wu et al., 2019). (2) NHEJ constitutes the preferential mechanism for the repair of double-strand breaks (DSBs) in primitive HSCs (Naka and Hirao, 2011). (3) Compared to HR, the efficacy of NHEJ is enhanced in FA cells (Du et al., 2016; Pace et al., 2010).

Although NHEJ is an error-prone DSB-repair mechanism that has been mainly used for gene knockout, this pathway could also be positively exploited to generate compensatory mutations that may restore FANCA functions, mimicking natural reversions described in mosaic FA patients. We thus hypothesized that the generation of insertion and/or deletion (indel) events in the vicinity of pathogenic mutations might constitute a gene-editing approach that would be particularly efficient for correcting the phenotype of HSCs from patients with FA. Due to the efficiency and versatility of the CRISPR/Cas9 system (Ran et al., 2013), we focused on this technology to investigate the efficacy of NHEJ to correct the phenotype of human FA hematopoietic cells harboring mutations in genes encoding for FA proteins involved in different steps of the FA pathway.

Our results show for the first time the feasibility of conducting NHEJ-editing-mediated correction of FA lymphoblastic cell lines (LCLs) from different complementation groups. Additionally, we demonstrate that this approach also confers phenotypic correction and proliferative advantage in $CD34^+$ cells from FA-A patients without compromising the repopulating properties of the self-renewing HSCs, suggesting that this very simple and versatile gene-editing approach should have a marked impact in the therapy of several monogenic diseases affecting the hematopoietic system.

RESULTS

Efficient NHEJ-Mediated Restoration of the FA Pathway in FA-A LCLs Harboring Different Biallelic Mutations in *FANCA*

In a first set of experiments, we investigated whether NHEJ could be exploited to correct FA-A cells with a biallelic insertion of a single nucleotide (c.3558insG) in exon 36 of *FANCA*. This insertion produces a 28-amino-acid frameshift, generating a premature stop codon (p.R1187EfsX28) (Castella et al., 2011). Notably, the spontaneous reversion of this mutation has been observed in several mosaic FA patients (Waisfisz et al., 1999), suggesting that slight variations in this FANCA domain could preserve the protein function.

Two different small guide RNAs (sgRNAs) were cloned separately into the all-in-one pX330 plasmid (Table S1) and electroporated in a FA-A patient LCL (FA-178) carrying the *FANCA* c.3558insG mutation in homozygosis (Table S2). Since the gINS11 generated a higher indel rate in FA-178 cells (data not shown), this sgRNA was selected for further experiments. Next-generation sequencing (NGS) analysis performed 5 days after gINS11 electroporation showed the occurrence of potentially therapeutic frame-restoring NHEJ-repair events at a frequency of 7.62%, while non-therapeutic indels occurred less frequently (2.32%) (Figure 1A).

To determine whether the putative therapeutic indels restored the functionality of the gene, different approaches were conducted. First, cells were maintained in culture and NGS analyses were performed at day 30 of incubation. These analyses showed a marked enrichment of therapeutic indels (from 7.62% to 16.45%), mainly due to the expansion of the 3′-guanine deletion immediately adjacent to the Cas9 cutting site (c.3579delG), while other indels disappeared (Figure 1A, right charts). This observation revealed that not all potentially therapeutic indels conferred proliferative advantage, suggesting that the open reading frame (ORF) restoration may not be sufficient to recover gene function. Protein BLAST analyses demonstrated the highly conserved nature of *FANCA* exon 36, confirming that c.3579delG was the only therapeutic indel that did not disrupt this conserved domain (Figure S1). Western blot analysis showed the restored expression of FANCA protein in edited cells (Figure 1B). Moreover, since FANCA is essential for FANCD2 recruitment to damaged DNA, FANCD2 immunofluorescence analyses were conducted in edited and unedited FA-178 cells to confirm the functionality of this

Figure 1. NHEJ-Mediated Gene Correction of a *FANCA* Frameshift Mutation (c.3558insG) in a FA LCL (FA-178) Nucleofected with gINS11 Nuclease

(A) Percentage of indels identified by NGS 5 and 30 days after gene editing. *FANCA* sequences were classified into three groups: edited sequences that restored the ORF (therapeutic indels: green), edited sequences that did not restore the ORF (other indels: red), and not edited alleles (unedited: gray). The different therapeutic indels identified in FA cells are listed (right panel). The guide recognition sequence and the predicted DSB site are marked with a purple line and a triangle, respectively. Black dashed line indicates the PAM sequence. Codons are represented alternating bold and normal letters. HD, healthy donor LCL; asterisk, used to align the sequences; dash, deleted nucleotide. Indels were named considering the mutated sequence as the reference one.

(B) Western blot analysis against FANCA confirmed the re-expression of this protein in edited FA cells. Vinculin was used as a loading control.

(C) NHEJ-mediated gene editing restored nuclear FANCD2 foci formation in edited FA. Top panel: representative FANCD2 immunofluorescence (Alexa-Fluor 594 nm) microphotographs. Bottom panel: percentage of cells with FANCD2 foci in the presence or absence of MMC. Bars represent mean ± SD.

(D) Reversion of MMC hypersensitivity in edited FA. Data are represented as mean ± SD.

(E) Restored chromosomal stability of edited FA cells after exposure to DEB. Top panel: representative microphotographs of the metaphases. Red arrows highlight specific aberrations. Bottom panel: percentage of aberrant cells in the absence (–) or presence (+) of DEB.

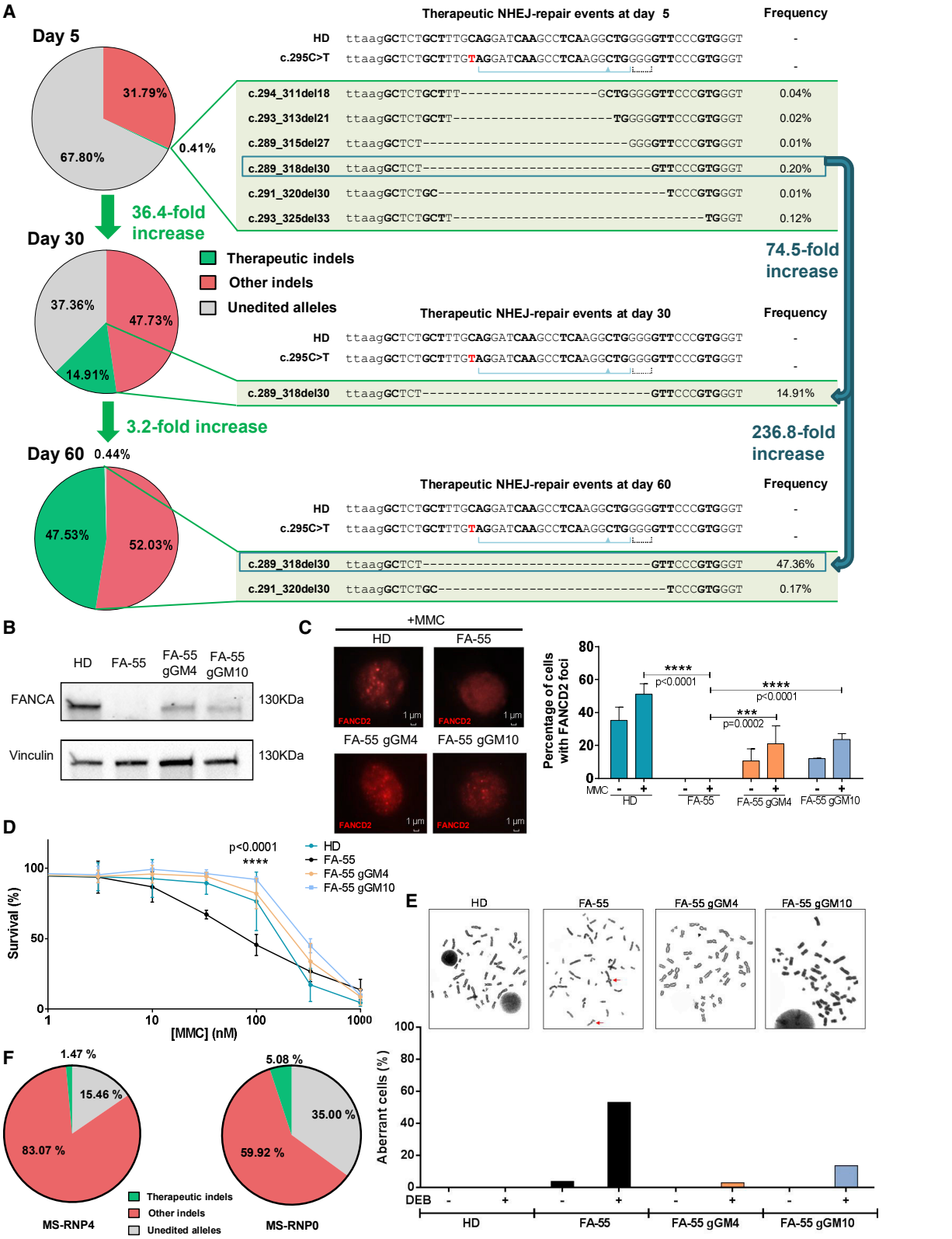

(legend on next page)

newly expressed FANCA protein. As shown in Figure 1C, edited cells displayed evident FANCD2 foci, particularly after exposure to mitomycin C (MMC), mimicking the behavior of healthy donor (HD) LCLs, thus confirming the restoration of the FA pathway in FA-A cells. To further demonstrate the correction of the FA-phenotype, edited cells were cultured in the presence of increasing doses of MMC. While unedited FA-178 LCL showed the characteristic hypersensitivity of FA cells to MMC, edited cells showed a marked increase in the resistance to this drug, behaving as HD cells (Figure 1D). Importantly, the correction of the chromosomal instability induced by diepoxibutane (DEB), a hallmark of FA, was also demonstrated in edited FA-178 cells both by analyses of chromosomal breaks (Figure 1E) and by the generation of micronuclei in these cells (Figure S2A). Finally, because the generation of reactive oxygen species (ROS) is increased in FA cells (Joenje et al., 1981), we also analyzed differences in ROS production between edited and untreated FA-178 cells. The fluorogenic test showed a significant reduction in ROS levels in edited compared to unedited cells (Figure S2B).

Neither NGS sequencing nor functional studies in unedited FA-178 (cultured in parallel to edited cells) showed evidence of spontaneous reversion of the c.3558insG mutation (not shown). This observation, together with the presence of editing events exclusively in the region that is close to the Cas9 cleavage site discarded spontaneous reversion of edited cells.

Taken together, these studies demonstrated the restored FA pathway and phenotypic correction of a FA-A LCL using a simple NHEJ-editing approach.

To confirm the efficacy of NHEJ to restore the function of *FANCA* mutations, we focused on the most frequent mutation described in FA patients from Spain. This mutation consists of a homozygous c.295C > T substitution in exon 4 that generates a premature stop codon, thus leading to a truncated, non-functional FANCA protein (p.Q99X) (Castella et al., 2011). This is a challenging mutation since the therapeutic NHEJ-mediated editing of these cells would require both the removal of the premature stop codon and also the preservation of the ORF, without disrupting any functional domain of FANCA. In contrast to the c.3558insG mutation, the reversion of c.295C > T has not been reported in FA patients (Callén et al., 2005).

As conducted with the c.3558insG mutation, two different sgRNAs were tested in patient-derived LCL (FA-55), both of which rendered a similar efficiency to generate indels in this target site of *FANCA* (around 30%) (Figures 2A and S3A). As expected from the complexity of the c.295C > T mutation, the initial frequency of therapeutic events was markedly lower (0.41% for gGM10 and 0.29% for gGM4; Figures 2A and S3A, respectively) as compared to efficacies observed in the LCL harboring the c.3558insG mutation (7.62%; Figure 1A). Nevertheless, 237- and 170-fold increases in the proportion of edited cells were observed 60 days after electroporation of FA-A LCLs with gGM10 and gGM4 nucleases, respectively (Figures 2A and S3A). Increases were even higher, when edited LCLs were expanded in the presence of MMC (Figure S3A).

NGS analyses showed that the proliferative advantage observed in these cells was mainly due to 30- and 33-bp deletions that were respectively generated with the gGM10 (c.289_318del30) and gGM4 (c.293_325del33) nucleases (Figures 2A and S3A, right panels). Strikingly, the frequency of other non-therapeutic indels was also increased over time (Figure 2A, red color). The Sanger sequencing of individual cell clones clarified that, while one of the *FANCA* alleles had been repaired by therapeutic NHEJ, the other allele harbored a non-therapeutic NHEJ-repair event (Figure S3B) that was expanded in parallel to the therapeutic indel, explaining the expansion of those non-therapeutic events.

Western blot analyses in edited FA-55 LCL pools and in seven edited clones confirmed the re-expression of FANCA, regardless of the therapeutic indel that occurred in these cells (Figures 2B and S3C). As previously observed with the c.3558insG mutation, the newly expressed FANCA protein in FA-55 cells was functional. This was deduced from many different phenotypic analyses carried out in edited cells, which evidenced restored formation of FANCD2 foci (Figure 2C), increased resistance to MMC (Figure 2D), reduced chromosomal fragility upon DEB challenge (Figure 2E; Figure S3D), and reduced ROS levels in edited cells (Figures S3E).

To improve the editing efficiency to target this challenging mutation, the CRISPR/Cas9 delivery system was modified. Instead of using a plasmid system, a ribonucleoprotein complex (RNP) composed of a chemically modified sgRNA4 containing, 2′-*O*-methyl 3′phosphorothioate (MS-sgRNA4) and Cas9 protein was used. As a result, the total frequency of indels, and also of potentially therapeutic indels were markedly increased (2.8- and 5.1-fold increase, respectively; Figure 2F, left chart) compared to values obtained with the plasmid Cas9 system (Figure S3A). Furthermore, the design of a new sgRNA (gGM0) that targets *FANCA* upstream and near the mutation (Table S1) markedly increased the frequency of therapeutic indels (up to 17.5-fold increase with respect to plasmid system; Figures 2F, right chart, S3F and S3G). These results demonstrate that NHEJ-mediated gene editing can be efficiently used for the generation of compensatory mutations capable of rescuing the

Figure 2. NHEJ-Mediated Correction of a Stop Codon Mutation (c.295C > T) in FA-55 LCL and Improvement of Editing Efficiency by Using a More Specific sgRNA (gGM0)

(A) Percentage of indels identified by NGS 5, 30, and 60 days after gene editing. The sequences obtained in the NGS were classified as in Figure 1.

(B) Western blot analysis showing the re-expression of FANCA in edited FA cells. Vinculin was used as a loading control.

(C) Restored FANCD2 foci formation in edited FA-55 cells. Left panel: representative immunofluorescence of FANCD2 foci. Right panel: percentage of cells with FANCD2 foci in the presence or absence of MMC. Bars represent mean ± SD.

(D) Correction of MMC sensitivity in edited FA cells. Data are represented as mean ± SD (n = 3).

(E) Restored chromosomal stability of edited FA cells exposed to DEB. Top panel: representative microphotographs of metaphases. Red arrows highlight specific aberrations. Bottom panel: percentage of aberrant cells in the absence and the presence of DEB.

(F) Editing efficiency in FA cells after nucleofection with MS-RNP4 (left) or with MS-RNP0 (right) designed for cleaving *FANCA* 2 nucleotides upstream the c.295 C > T mutation (n = 3).

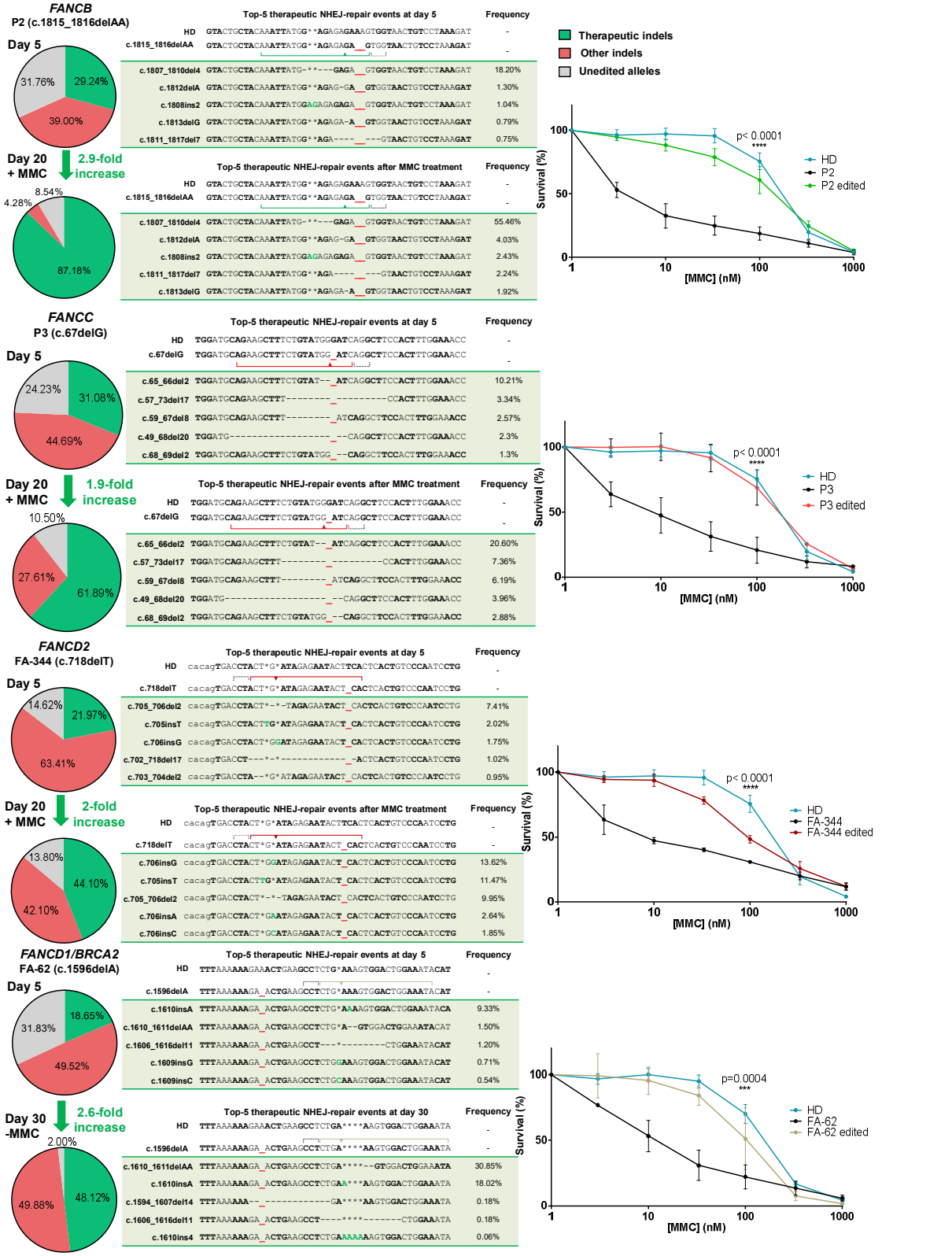

(legend on next page)

function of FANCA, not only in easy-to-repair but also in complex *FANCA* mutations.

Therapeutic NHEJ-Mediated Editing of Different FA Complementation Groups

To study the feasibility of using NHEJ editing to correct mutations in other FA complementation groups, LCLs with mutations in other FA genes were selected. Particularly we used cells harboring mutations in genes encoding for proteins that participate in different complexes of the FA pathway: upstream (FANCB, FANCC), intermediate FA-D2/I (FANCD2), and downstream (BRCA2) (Table S2). A unique sgRNA was designed per mutation, prioritizing the score and the proximity to the mutation (Table S1). In all instances, RNP complexes including the MS-sgRNAs and the Cas9 protein (MS-RNPs) were electroporated in the different LCLs. As shown in Figure 3, average editing efficiencies in all the FA LCLs were 74.39% ± 8.15%, with potential therapeutic indels ranging from 18.65% to 31.08%, measured by NGS 5 days after nucleofection. In all instances, the percentage of cells with potentially therapeutic indels was increased when edited cells were incubated, in either the absence or the presence of MMC, suggesting the correction of the pathogenic mutation. Importantly, the analysis of MMC sensitivity confirmed in all cases the correction of the characteristic MMC hypersensitivity of FA-B, FA-C, FA-D2, and FA-D1 cells after NHEJ editing (Figure 3, right panels).

These results confirm that NHEJ-mediated repair is a simple and efficient system to correct mutations in different FA complementation groups, including cells with mutations in *FANCD1/BRCA2*, characterized by a marked defect in HR.

FANCA NHEJ-Mediated Gene Editing in Hematopoietic Repopulating Cells from Healthy Human Donors

Once we demonstrated that NHEJ corrected the phenotype of LCLs from different FA patients' complementation groups, we investigated the feasibility of using this strategy to edit *FANCA* in human HSCs, which is the preferential target population for the hematopoietic treatment of FA patients. To evaluate whether the NHEJ editing of *FANCA* was compatible with the preservation of the repopulating properties of human HSCs, initial experiments were conducted in which HD cord blood $CD34^+$ cells were electroporated with a RNP composed by the Cas9 protein complexed with either an *in vitro*-transcribed sgRNA4 (IVT-RNP4) or with a chemically modified version of this guide (MS-RNP4). As shown in Figure 4A, a much higher percentage of indels was observed when the MS-RNP4 nuclease was used (87.8% ± 4.8% indels), as compared with the IVT sgRNA (13.2% ± 10.2% indels). Notably, the analysis in different $hCD34^+$ subpopulations showed similar editing efficiencies in all cases, even in the very primitive $CD34^+CD133^+CD90^+$ precursors, suggesting that NHEJ editing efficiently targets the self-renewing HSCs (Figure 4B).

To corroborate these results and to investigate the impact of the gene editing mediated by the MS-RNP4 nuclease in long-term repopulating HSCs, transplantation studies were conducted in immunodeficient mice. Since the targeting of *FANCA* with this nuclease might generate not only monoallelic but also biallelic DSBs in this gene, these experiments would also allow us to investigate in parallel, the repopulating properties of human HSCs from the same donor harboring unedited or edited HSCs, either in one or the two *FANCA* alleles. Thus, based on the recessive nature of the disease, edited cells harboring two biallelic truncating mutations in *FANCA* would behave as FA-like cells.

Analysis of the percentage of human cells ($hCD45^+$ cells) in primary recipients that had been transplanted with either MS-RNP4-nucleofected cells (MS-RNP4), or the two control groups, not nucleofected (control) and mock-nucleofected cells (mock), showed very high and similar levels of engraftment. In all instances, levels of engraftment in the BM of transplanted mice ranged between 70% and 85% (Figure 4C) and showed similar levels of engraftment in the different hematopoietic subpopulations (Figures 4C and S4A–S4C). Moreover, re-transplants carried out in secondary recipients confirmed the long-term repopulating and multi-lineage differentiation ability of MS-RNP4-nucleofected cells (Figures 4D, S4D, and S4F). However, in these secondary recipients, lower though non-significantly different levels of engraftment were observed in the MS-RNP4 group (16.8% ± 12.2% $CD45^+$ cells in BM), as compared to the control (44.1% ± 31.5%) and mock (36.1% ± 26.9%) groups (Figures 4D), probably due to the generation of biallelic mutations in a percentage of transplanted HSCs (see details in Figure 5).

To comparatively investigate the efficiency of NHEJ editing mediated by the MS-RNP4 nuclease in hematopoietic committed progenitor cells, versus primitive HSCs that repopulated the hematopoiesis of immunodeficient mice, NGS analyses were carried out in samples corresponding to Figure 4, both in the bulk of $CD34^+$ cells prior to transplantation and also in human hematopoietic cells that repopulated the BM of primary and secondary recipients (Figure 5A). Although in most cases no significant differences were observed in indel levels in the bulk population of $CD34^+$ cells (87.8% ± 4.8% indels) and in long-term repopulating cells (57.97% ± 34.22%), a decreasing trend was observed. For this reason, we investigated the frequency of the different type of editing events found in the pool of $CD34^+$ cells compared to those observed in the BM cells. Two different types of *FANCA*-editing events may take place in these cells: in-frame indels (potentially non-pathogenic) or truncating indels (which would result in a FA-like cell phenotype in cells harboring biallelic mutations) (Figure 5B). Interestingly, the frequency of truncating indels was markedly decreased after transplantation, suggesting that many of these truncating mutations took place in both alleles of the repopulating cells. In marked contrast with this observation, the frequency of in-frame indels observed in the pool of

Figure 3. NHEJ-Mediated Phenotypic Correction of LCLs Corresponding to Four Different FA Complementation Groups

Efficacies of gene correction and reversion of MMC hypersensitivity were tested in FA-B, FA-C, FA-D2, and FA-D1 with biallelic mutations in *FANCD1/BRCA2*. Left panels: the pie charts indicate the percentage of indels identified by NGS 5 days after electroporation and after 20–30 days of *in vitro* culture in the presence (FA-B, FA-C, and FA-D2) or the absence (FA-D1) of 100 nM MMC. Sequences obtained by NGS were classified as in Figure 1. In those cases where the original mutation was a deletion, indels were named considering the mutated sequence as the reference one. Right panels show the correction of the MMC hypersensitivity characteristic of FA LCLs. Data are represented as mean ± SD (n = 3).

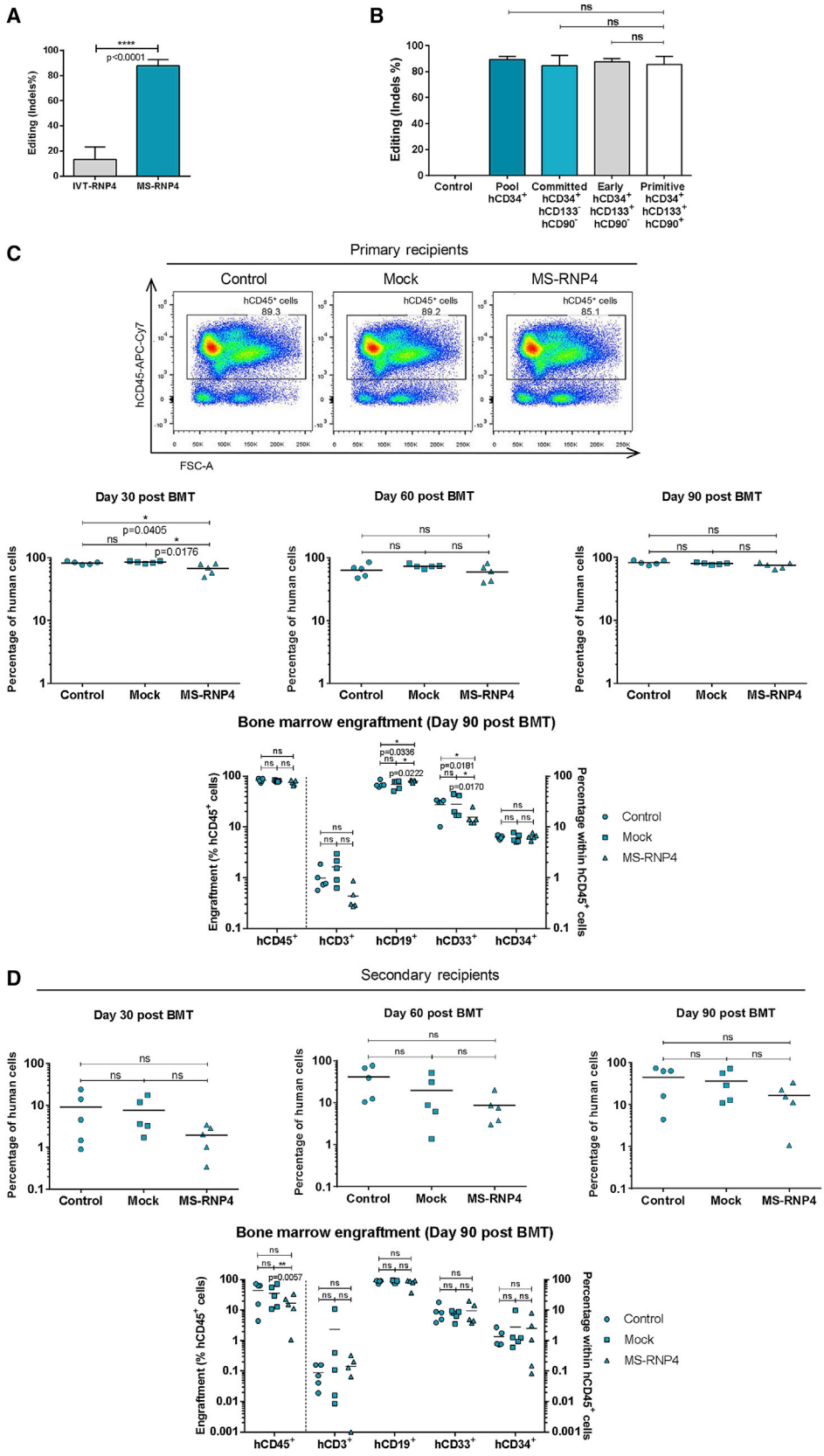

(legend on next page)

$CD34^+$ cells was maintained in cells that repopulated either primary or secondary recipients. Sanger sequencing of human hematopoietic colonies generated by nucleofected cells, either before or after transplantation, allowed us to deeply investigate the different phenotypes of the respective progenitor cells: FA-like, thus carrying biallelic truncating mutations in *FANCA* or HD-like edited cells carrying at least one WT allele or one allele harboring an in-frame indel. Such in-frame indels could thus be potentially therapeutic if generated in FA cells, as will be described in experiments corresponding to Figures 6 and 7. Remarkably, the majority of the colonies generated by electroporated $CD34^+$ cells harbored editing events (97.2%), most of which resulted in an FA-like phenotype (74.6%), while 22.6% of the edited colonies consisted of HD-like cells (Figure 5C). In clear contrast to this observation, the repertoire of editing events markedly changed when clonogenic assays were generated by human progenitors that repopulated primary or secondary recipients. In these colonies, the HD-like cells were the predominant populations, while the presence of FA-like cells almost completely disappeared, consistent with the repopulating defect of FA cells, and thus with the proliferative advantage of edited HD-like cells. Strikingly, the increase in the percentage of unedited cells *in vivo* was also higher than HD-like cells, suggesting that some of the in-frame indels generated in HD-like cells were not "neutral" mutations and thus not as efficient in terms of repopulation as the WT sequence.

The analysis of the most frequent indels (top 20) determined before transplantation and at different time points post-transplantation showed that a reduced proportion of indels (23.8%; Figure 5D and Table S3, Code A) were detected both before and after transplantation. The high frequency of the c.311delG and c.311insG mutations is probably due to the higher probability of generating small indels closed to the cutting site (Canver et al., 2014)). Other indels were more frequently represented only long term after transplantation, suggesting a potentially non-pathogenic nature of these editing events (Figure 5D; Table S3).

Altogether these results demonstrate that NHEJ editing efficiently targets the long-term repopulating HSCs and show that a significant number of the editing events in *FANCA* are compatible with the preservation of the repopulating properties of the HSCs.

Therapeutic NHEJ Gene Editing of Hematopoietic Progenitor and Repopulating Cells from FA-A Patients

As a proof of concept, we investigated the feasibility of correcting the phenotype of HSPCs from FA-A patients carrying the homozygous pathogenic c.295C > T mutation by means of NHEJ-mediated gene editing. Thus, BM and mobilized peripheral blood (mPB) $CD34^+$ cells from three FA-A patients were edited with the IVT-RNP4 nuclease.

Figure 6A shows the results corresponding to the editing of BM $hCD34^+$ cells from patient FA-807. In this case, an indel rate of 23.33% was determined at day 5 post-electroporation; 15.35% corresponded to non-therapeutic indels and 7.98% to therapeutic indels, most of which (7.84% in total) harbored a specific 30-bp deletion. Twenty-four hours after electroporation, clonogenic assays were also conducted, both in the absence and the presence of MMC. The analysis of individual colonies generated in the absence of MMC showed that 50% of the colonies were positive for the presence of therapeutic indels (Figures 6A, bottom panel, and S5A). Most of the edited colonies (92.3% of them) harbored the c.289_318del30 deletion previously shown to be functional in FA-A-edited LCLs clones (Figure S3B), representing a 5.9-fold increase with respect to the frequency determined by NGS in $hCD34^+$ cells at day 5 post-electroporation (7.84%). Significantly, when Sanger sequencing was conducted in individual colonies grown in the presence of 3 and 10 nM MMC, a progressive increase in the proportion of colonies carrying this 30-bp deletion was observed, reaching 100% of colonies when 10 nM MMC was used (Figures 6A, bottom panel, and S5).

We then used mPB $CD34^+$ cells from FA patients, the main source of HSCs currently used in gene therapy clinical trials. When $CD34^+$ cells from patient FA-807 were edited with the IVT-RNP4 nuclease and analyzed by NGS at day 5 post-electroporation, 16.84% of total indels were determined, being the proportion of non-therapeutic and therapeutic indels of 14.19% and 2.65%, respectively (Figure 6B, top panel). Once again, most of the therapeutic indels (2.64%) corresponded to the c.289_318del30 deletion. The analysis of colonies generated after nucleofection showed that 25% of them contained therapeutic indels (10-fold higher compared to day 5 post-nucleofection). In this case, all colonies with therapeutic indels harbored the 30-bp deletion (Figure 6B, bottom panel), in good consistency with data obtained in previous analyses (Figures 2 and S3).

A new experiment was then conducted with mPB $hCD34^+$ cells from another FA patient (FA-739). After electroporation with IVT-RNP4, an indel rate of 12.32% was determined at day 5 post-electroporation, being the proportion of therapeutic indels 0.45% (Figure 6C, top panel). When these cells were maintained in culture for 14 days, the proportion of total therapeutic indels increased 5-fold (2.33%) (Figure 6C, bottom

Figure 4. Preserved Repopulating Properties of HD $CD34^+$ Cells after *FANCA* NHEJ-Mediated Editing with MS-sgRNA Nucleases

(A) Improved NHEJ-mediated editing with an RNP nuclease composed by a MS-sgRNA Cas9 protein (MS-RNP4) compared to the IVT sgRNA nuclease (IVT-RNP4; 4 and 6 independent experiments were conducted with each nuclease. Bars represent mean ± SD).

(B) High and similar editing efficacies in different HSPC subpopulations edited with the MS-RNP4. Bars represent mean ± SD (n = 3).

(C) Preserved repopulating properties of $hCD34^+$ cells edited with the MS-RNP4 in primary NSG recipients. Top panel: representative dot plot analysis showing the engraftment of human $CD45^+$ cells in the BM of NSG recipients 90 days after transplantation of not nucleofected HD $hCD34^+$ cells (control) or with $CD34^+$ cells nucleofected without nuclease (Mock) or nucleofected with the MS-RNP4 nuclease (MS-RNP4). Center panels represent the percentages of human engraftment ($hCD45^+$) in BM. The bottom panel shows multi-lineage engraftment levels in primary recipients transplanted with unedited and edited $hCD34^+$ cells. Multi-lineage reconstitution was evaluated using antibodies against hCD3 for T cells, hCD19 for B cells, hCD33 for myeloid cells, and hCD34 for HSPCs. Data are represented as mean ± SD (n = 5 in each group).

(D) Analysis of the long-term hematopoietic repopulating ability of edited $hCD34^+$ in secondary recipients transplanted with BM cells from primary recipients shown in (C). Secondary recipients were transplanted with total BM obtained from each primary mouse (mouse to mouse). Data are represented as mean ± SD (n = 5 in each group). BMT, bone marrow transplantation.

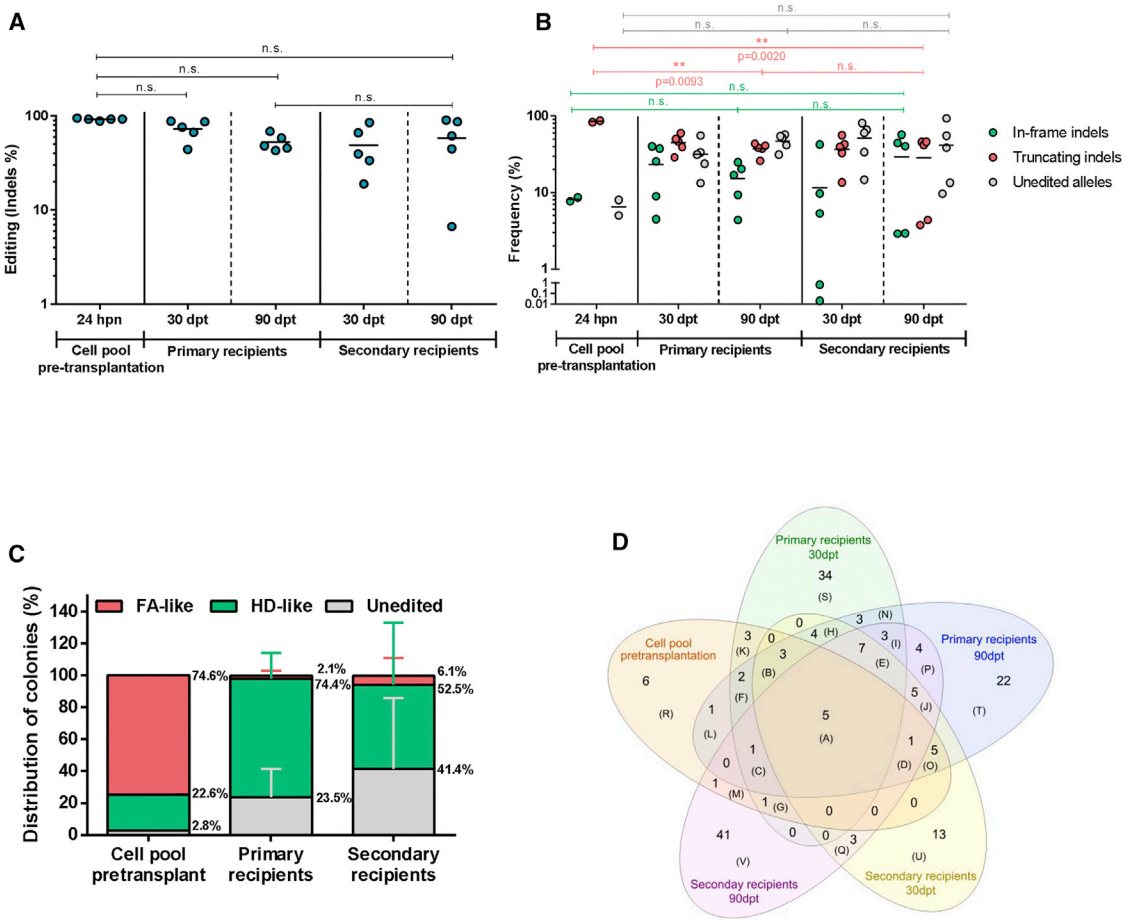

Figure 5. Efficient NHEJ-Mediated Gene Editing of *FANCA* in HD Long-Term Hematopoietic Repopulating Cells

(A) Comparative analysis of the editing efficiency in HD hematopoietic cells prior to (data from Figure 4A) and after transplantation of HD hCD34$^+$ cells nucleofected with MS-RNP4 nuclease (MS-RNP4). No significant differences were observed in the editing frequency between primary hCD34$^+$ cells and hematopoietic cells obtained from either primary or secondary NSG recipients. Data are represented as mean ± SD (n = 5 in each group).

(B) Analysis of the frequency of in-frame and truncating indels determined in human hematopoietic cells prior to and after transplantation in primary and secondary recipients. Each symbol identifies a recipient. Alleles were classified as in-frame indels (that potentially preserve FANCA function; green), truncating indels (interrupting the ORF; red), and unedited alleles (gray). Data are represented as mean ± SD (n = 5 in each group).

(C) Distribution of human hematopoietic colonies harboring biallelic truncating mutations in *FANCA* (FA-like; red) or mutations in which at least one allele is WT or harbors an in-frame mutation (HD-like; green). Colonies without indels are marked in gray. Human hematopoietic colonies generated by CD34$^+$ cells prior to transplantation or from the BM of primary and secondary recipients are shown. In all instances, colonies were sequenced by Sanger. Bars represent mean ± SD.

(D) Venn diagram showing the top 20 indels found in the CD34$^+$ cell pool prior to transplantation and in the different primary and secondary recipient mice after transplantation. The number of common and specific indels identified in the different tested populations is shown.

panel). NGS analysis confirmed that cells harboring the c.289_318del30 deletion experienced a preferential growth advantage, with a 55.3-fold increase from 5 to 14 days post-electroporation.

Finally, the analysis of the *in vitro* differentiation capacity of CD34$^+$ cells from FA-A patients showed that NHEJ-mediated editing does not affect the erythroid and myeloid differentiation capacity (Figure S6).

To assure the specificity and safety of our sgRNA in FA-HSPCs, the top five and top twenty *in silico* predicted off-target loci were analyzed by NGS in edited FA-A and HD HSPCs, respectively. Importantly, no significant unspecific nuclease activity was detected in any of the off-target loci studied (Figure S7).

Once demonstrated the efficiency and safety of NHEJ-mediated gene editing in the pool of FA CD34$^+$ cells and in their clonogenic progenitor cells, we investigated the possibility of editing repopulating cells from another FA-A patient that harbored the c.295C > T mutation (FA-655). In this case, 24 h after IVT-RNP4-electroporation cells were used both for establishing clonogenic assays and for the transplantation of one NSG mouse (Figure 7). While 10% of the 56 colonies analyzed harbored indels, no therapeutic events were identified in this case, indicating that the frequency of therapeutic indels in these CFCs should be lower than 1.8%, which would correspond to a detection limit of 1 positive colony out of 56 colonies (Figure 7A). Strikingly, NGS analyses conducted in the BM of the transplanted mouse (30 days post-infusion)

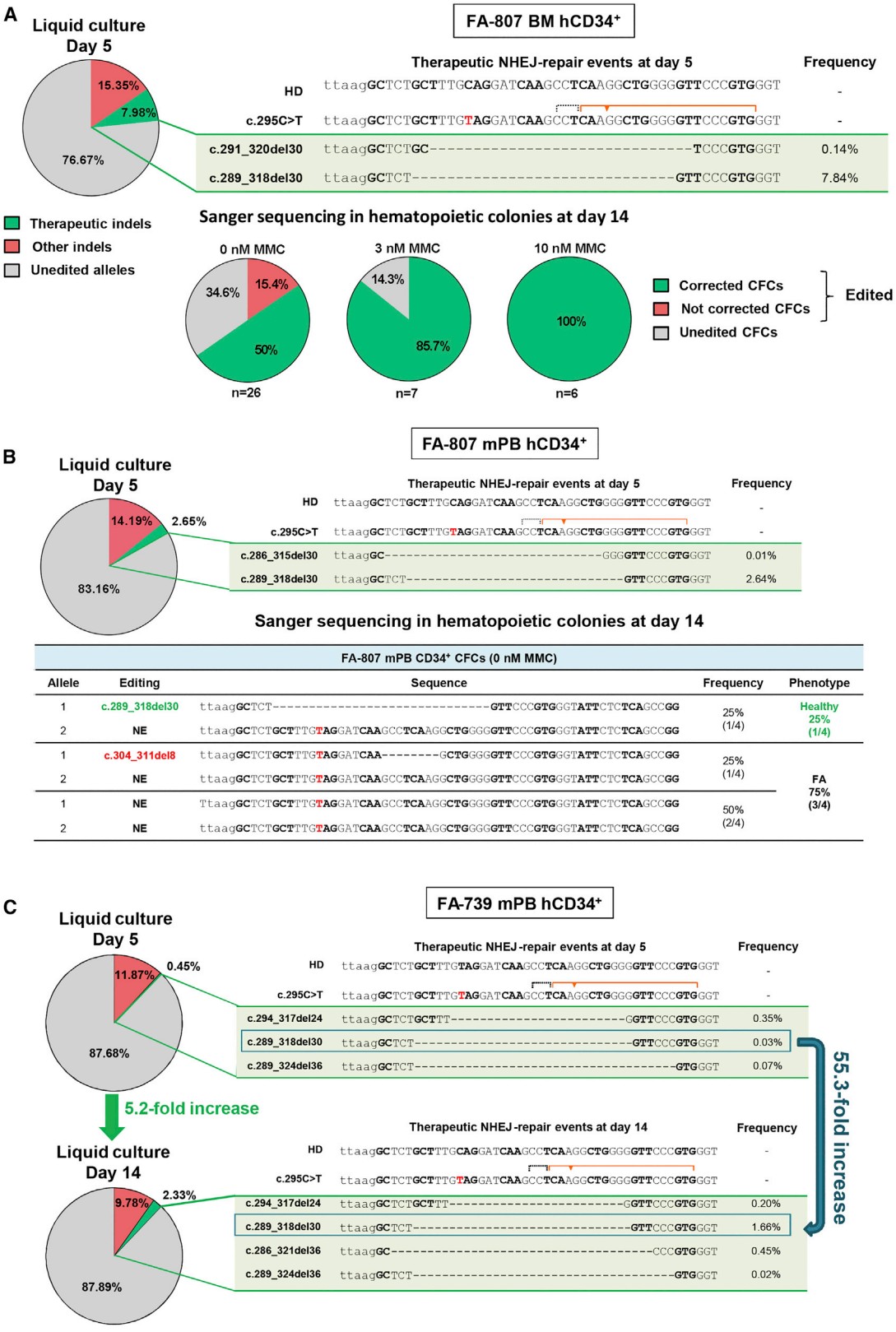

(legend on next page)

A

FA-655 mPB hCD34⁺ **Sanger sequencing in hematopoietic colonies at day 14**

FA-655 mPB CD34⁺ CFCs (0 nM MMC)				
Allele	Editing	Sequence	Percentage	Phenotype
1	NE	ttaagGCTCTGCTTTGTAGGATCAAGCCTCAAGGCTGGGGGTTCCCGTGGGTATTCTCTCAGCCG	75% (42/56)	FA 100% (56/56)
2	NE	ttaagGCTCTGCTTTGTAGGATCAAGCCTCAAGGCTGGGGGTTCCCGTGGGTATTCTCTCAGCCG		
1	NE	ttaagGCTCTGCTTTGTAGGATCAAGCCTCAA*GGCTGGGGGTTCCCGTGGGTATTCTCTCAGCC	7.1% (4/56)	
2	c.310insG	ttaagGCTCTGCTTTGTAGGATCAAGCCTCAAGGGCTGGGGGTTCCCGTGGGTATTCTCTCAGCC		
1	NE	ttaagGCTCTGCTTTGTAGGATCAAGCCTCAAGGCTGGGGGTTCCCGTGGGTATTCTCTCAGCCG	8.9% (5/56)	
2	c.315delG	ttaagGCTCTGCTTTGTAGGATCAAGCCTCAA*GGCT-GGGGTTCCCGTGGGTATTCTCTCAGCC		
1	NE	ttaagGCTCTGCTTTGTAGGATCAAGCCTCAAGGCTGGGGGTTCCCGTGGGTATTCTCTCAGCCG	1.8% (1/56)	
2	c.313_316del4	ttaagGCTCTGCTTTGTAGGATCAAGCCTCAAGG----GGGTTCCCGTGGGTATTCTCTCAGCCG		
1	NE	ttaagGCTCTGCTTTGTAGGATCAAGCCTCAAGGCTGGGGGTTCCCGTGGGTATTCTCTCAGCCG	1.8% (1/56)	
2	c.311_316del7	ttaagGCTCTGCTTTGTAGGATCAAGCCTCA-------GGGTTCCCGTGGGTATTCTCTCAGCCG		
1	NE	ttaagGCTCTGCTTTGTAGGATCAAGCCTCAAGGCTGGGGGTTCCCGTGGGTATTCTCTCAGCCG	1.8% (1/56)	
2	c.311_320del11	ttaagGCTCTGCTTTGTAGGATCAAGCCTCA----------TCCCGTGGGTATTCTCTCAGCCG		
1	NE	ttaagGCTCTGCTTTGTAGGATCAAGCCTCAAGGCTG***GGGGTTCCCGTGGGTATTCTCTCAG	1.8% (1/56)	
2	c.315ins3	ttaagGCTCTGCTTTGTAGGATCAAGCCTCAAGGCTGATCGGGGTTCCCGTGGGTATTCTCTCAG		
1	c.315delG	ttaagGCTCTGCTTTGTAGGATCAAGCCTCAAGGCT-GGGGTTCCCGTGGGTATTCTCTCAGCCG	1.8% (1/56)	
2	c.298_339del43	ttaagGCTCTGCTTTGTA----------GCCG		

B

Figure 7. *In Vivo* Proliferative Advantage of mPB HSPCs from a FA-A Patient after NHEJ-Mediated Gene Editing

CD34⁺ cells harboring the truncating c.295C > T mutation in *FANCA* from FA-655 patient mPB were electroporated with IVT-RNP4 and then used for establishing clonogenic assays and for the transplantation of one NSG mouse.

(A) Analysis of the editing events in individual colonies using Sanger sequencing (a total of 56 colonies were analyzed).

(B) NGS analysis of the editing events in human hematopoietic cells engrafting the BM of the transplanted NSG mouse, 1 month after transplantation.

showed that 17.31% of the human engrafted cells harbored editing events at the target site. Specifically, 8.28% of the editing events corresponded to the therapeutic c.289_318del30 deletion (Figure 7B), revealing the engraftment and *in vivo* proliferative advantage of FA-A hematopoietic repopulating cells that were genetically corrected by means of a NHEJ-mediated gene therapy approach.

DISCUSSION

Several studies have shown the feasibility of HR-mediated gene editing as a novel approach to correct HSPCs from patients affected by inherited and acquired diseases (De Ravin et al., 2016; Dever et al., 2016; Genovese et al., 2014; Hoban et al., 2015; Pavel-Dinu et al., 2019). In contrast to HR, NHEJ repair

Figure 6. *In Vitro* Proliferative Advantage of FA-A Patients' HSPCs Harboring the c.295C > T Mutation after Therapeutic NHEJ-Mediated Gene Editing

Human CD34⁺ cells from patients FA-807 and FA-739 harboring the truncating c.295C > T mutation in *FANCA* were edited with the IVT-RNP4 nuclease. The efficiency of NHEJ-mediated editing was measured by NGS at day 5 in liquid culture and the proliferative advantage by Sanger sequencing in individual colonies generated after 14 days of culture in methylcellulose or by NGS of the liquid culture.

(A and B) Analysis of gene editing events measured by NGS in (A) BM and (B) mPB CD34⁺ cells from patient FA-807.

(C) Characterization of editing events in mPB CD34⁺ cells from patient FA-739 in liquid cultures both at 5 and 14 days post-nucleofection. Editing events were classified as in Figure 1.

has been mainly used to knock out specific genes due to the generation of indels disrupting the targeted gene. However, the feasibility of using NHEJ as a therapeutic alternative to restore the expression of mutated genes has also been described in Duchenne muscular dystrophy. In this disease model, exon skipping in the dystrophin gene has shown to partially correct the function of the gene (Ousterout et al., 2013, 2015a, 2015b). Very recently, NHEJ has also been used in myeloid cell lines targeting correction of a *CYBB* gene mutation introduced with lentiviral vectors (Sürün et al., 2018). In the field of FA, a similar approach has been used to correct *Fancf* in mouse fibroblasts (van de Vrugt et al., 2019). Despite these previous studies, NHEJ-based editing has never been applied to correct pathogenic mutations in human HSCs. Considering that NHEJ constitutes the preferred mechanism for the repair of DSBs, particularly in quiescent cells (Naka and Hirao, 2011), and taking into account that NHEJ is enhanced in FA cells (Du et al., 2016; Pace et al., 2010), we postulated that the NHEJ editing in HSCs from FA patients should constitute an ideal approach for the targeted correction of these cells.

The results presented in this study show for the first time the feasibility of correcting the phenotype of LCLs from FA patients carrying mutations in genes that encode for proteins participating in the different complexes of the FA pathway: upstream, intermediate, and downstream complex (particularly relevant for HR), confirming the versatility of the proposed editing strategy.

Importantly, our *in vitro* and *in vivo* studies showed that NHEJ-mediated editing efficiently targets the long-term HSCs. This contrasts with the reduced efficacy of HR for the editing of long-term repopulating cells, compared to efficacies achieved in more mature progenitor cells (Dever et al., 2016; Genovese et al., 2014; Hoban et al., 2015; Pavel-Dinu et al., 2019). Moreover, in contrast to HR, where the pre-stimulation of HSCs is essential to induce HR, NHEJ does not require this pre-stimulation step, thus preserving the stemness and, consequently, the repopulating ability of gene-edited HSCs. This hypothesis has been demonstrated in our studies shown in Figure 5B revealing that the NHEJ-editing efficacy obtained in the pool of HD CD34$^+$ cells was similar to the one corresponding to HSCs with HD-like phenotype. Indeed, this observation will have a particular relevance for the therapy of FA HSCs, characterized by a marked sensitivity to *in vitro* manipulation (Río et al., 2017).

Importantly, our editing studies in FA LCLs and FA CD34$^+$ cells have shown that some of the potential therapeutic editing events in *FANCA* are capable of re-expressing a functional FANCA. Moreover, our studies revealed the restoration of the FA pathway and also a marked proliferative advantage and phenotypic correction in edited cells. This proliferative advantage was particularly remarkable in the case of the complex c.295C > T stop codon mutation in which a striking proliferative advantage of FA-A HSPCs harboring therapeutic editing was observed not only in progenitor cells analyzed a few days after nucleofection (25%–50% editing rates) but also in NSG mice engrafting cells. Additionally, the fact that the same 30 bp deletion was frequently found both in FA LCLs and FA HSPCs, demonstrates the advantage of this event compared to other potential therapeutic events initially generated.

Because of recent optimizations described in the sgRNA design enabling increased stability *in vitro* (Bak et al., 2018; Brunetti et al., 2018) and the possibility of targeting sgRNAs near to the mutation, a marked increase in the indel rates has been achieved in our study. In this respect, the frequency of indels in both FA LCLs and CD34$^+$ cells were higher than 65%, with a frequency of therapeutic indels as high as 18%–31% in FA-LCLs (Figure 3). This increased efficiency together with the very simple and inexpensive design of new sgRNAs will assure the expansion of this approach for the correction of different mutations, not only in HSPC diseases (such as FA) in which edited cells will develop proliferation advantage but also in other monogenic blood disorders (Table S4). Nevertheless, aiming at the convenient development of therapies based on NHEJ-mediated editing, specific missense and frameshift mutations (small indels) that do not affect key protein domains should be preferentially selected. Finally, mutations not targetable by this approach could also benefit from the high efficiency of NHEJ-mediated repair in HSCs by the use of homology-independent targeted integration (HITI) strategies (Suzuki and Izpisua Belmonte, 2018).

In summary, our results demonstrate that NHEJ-based gene editing should constitute a simple therapeutic gene editing approach for the gene therapy of a specific group of patients harboring small mutations in genes accounting for a variety of monogenic lympho-hematopoietic diseases, including those attributable to mutations in many different genes, such as FA and Diamond-Blackfan anemia. Additionally, as opposed to conventional gene therapy or HR-mediated gene editing, NHEJ-mediated editing does not require the use of viral vectors, thus enormously reducing the complexity and cost of the therapy.

STAR★METHODS

Detailed methods are provided in the online version of this paper and include the following:

- KEY RESOURCES TABLE
- LEAD CONTACT AND MATERIALS AVAILABILITY
- EXPERIMENTAL MODEL AND SUBJECT DETAILS
  - Mice
  - Cell Lines
  - Hematopoietic stem and progenitor cells from healthy donors and FA patients
- METHOD DETAILS
  - Plasmids
  - Ribonucleoprotein complex
  - LCLs gene editing
  - Gene editing experiments in HD and FA-A HSPCs
  - LCLs single clone isolation
  - Colony Forming Unit Assay
  - Transplantation of Gene-edited Healthy donor and FA HSPCs in NSG mice
  - FANCA protein expression by Western-blot
  - Nuclear FANCD2 foci immunofluorescence
  - MMC sensitivity test
  - Chromosome Diepoxybutane Analysis

- Chromosome fragility by the flow cytometric micronucleus test
- Analysis of reactive oxygen species (ROS)
- NHEJ-repair events characterization by Sanger Sequencing
- CRISPR/Cas9-induced gene editing analysis by Inference of CRISPR Editing (ICE)
- CRISPR/Cas9-induced gene editing analysis by Next Generation Sequencing
- Next Generation Sequencing analysis of putative off-targets
- Potential mutations to be treated by NHEJ-mediated gene editing

- QUANTIFICATION AND STATISTICAL ANALYSIS
- DATA AND CODE AVAILABILITY

SUPPLEMENTAL INFORMATION

Supplemental Information can be found online at https://doi.org/10.1016/j.stem.2019.08.016.

ACKNOWLEDGMENTS

The authors would like to thank Jonathan Schwartz for critical reading of the manuscript, Aurora de la Cal for her assistance in coordinating patients' samples, and Miguel A. Martín and Sergio García for the maintenance and irradiation of the animals, respectively. This work was supported by "Ministerio de Economía, Comercio y Competitividad y Fondo Europeo de Desarrollo Regional (FEDER)" (SAF2015-68073-R, SAF2015-64152-R, and RTI2018-097125-B-I00), "7th Framework Program European Commission" (HEALTH-F5-2012-305421 and EUROFANCOLEN), "Ministerio de Sanidad, Servicios Sociales e Igualdad" (EC11/060 and EC11/550), "Fondo de Investigaciones Sanitarias, Instituto de Salud Carlos III" (RD12/0019/0023), ICREA-Academia program, and Rocket Pharmaceuticals Inc. R.T.-R. is supported by a postdoctoral fellowship from the Asociación Española Contra el Cáncer (AECC).

AUTHOR CONTRIBUTIONS

Conceptualization, F.J.R.-R., J.A.B., and P.R.; Methodology, F.J.R.-R., J.A.B., and P.R.; Investigation, F.J.R.-R., L.U., L.A., B.D., C.R., M.J.R., S.B., F.M., S.R.-P., and P.R.; Formal Analysis, F.J.R.-R., L.U., B.D., and P.R.; Resources, M.C., M.B., C.A., H.H., J. Sevilla, S.R.-P., J. Surrallés, and R.T.-R.; Writing – Original Draft, F.J.R.-R., J.A.B., and P.R.; Writing – Review & Editing, F.J.R.-R., L.U., B.D., J.A.B., and P.R.; Visualization, F.J.R.-R., L.U., B.D., J.A.B., and P.R., Project Administration, P.R.; Funding Acquisition, J.A.B. and P.R.; Supervision, J.A.B. and P.R.

DECLARATION OF INTERESTS

J.A.B. and J. Sevilla are consultants for Rocket Pharmaceuticals Inc. (RP). J.A.B. and P.R. have licensed gene therapy vectors to RP and have also obtained financial support from this company. J. Surrallés also receives funding from RP. The rest of the authors declare no competing financial interests.

Received: November 12, 2018
Revised: June 24, 2019
Accepted: August 26, 2019
Published: September 19, 2019

REFERENCES

Asur, R.S., Kimble, D.C., Lach, F.P., Jung, M., Donovan, F.X., Kamat, A., Noonan, R.J., Thomas, J.W., Park, M., Chines, P., et al. (2018). Somatic mosaicism of an intragenic FANCB duplication in both fibroblast and peripheral blood cells observed in a Fanconi anemia patient leads to milder phenotype. Mol. Genet. Genomic Med. *6*, 77–91.

Avlasevich, S.L., Bryce, S.M., Cairns, S.E., and Dertinger, S.D. (2006). In vitro micronucleus scoring by flow cytometry: differential staining of micronuclei versus apoptotic and necrotic chromatin enhances assay reliability. Environ. Mol. Mutagen. *47*, 56–66.

Bak, R.O., Dever, D.P., and Porteus, M.H. (2018). CRISPR/Cas9 genome editing in human hematopoietic stem cells. Nat. Protoc. *13*, 358–376.

Brunetti, L., Gundry, M.C., Kitano, A., Nakada, D., and Goodell, M.A. (2018). Highly Efficient Gene Disruption of Murine and Human Hematopoietic Progenitor Cells by CRISPR/Cas9. J. Vis. Exp. Published online April 10, 2018. https://doi.org/10.3791/57278.

Callén, E., Casado, J.A., Tischkowitz, M.D., Bueren, J.A., Creus, A., Marcos, R., Dasí, A., Estella, J.M., Muñoz, A., Ortega, J.J., et al. (2005). A common founder mutation in FANCA underlies the world's highest prevalence of Fanconi anemia in Gypsy families from Spain. Blood *105*, 1946–1949.

Canver, M.C., Bauer, D.E., Dass, A., Yien, Y.Y., Chung, J., Masuda, T., Maeda, T., Paw, B.H., and Orkin, S.H. (2014). Characterization of genomic deletion efficiency mediated by clustered regularly interspaced short palindromic repeats (CRISPR)/Cas9 nuclease system in mammalian cells. J. Biol. Chem. *289*, 21312–21324.

Castella, M., Pujol, R., Callén, E., Trujillo, J.P., Casado, J.A., Gille, H., Lach, F.P., Auerbach, A.D., Schindler, D., Benítez, J., et al. (2011). Origin, functional role, and clinical impact of Fanconi anemia FANCA mutations. Blood *117*, 3759–3769.

Charrier, S., Ferrand, M., Zerbato, M., Précigout, G., Viornery, A., Bucher-Laurent, S., Benkhelifa-Ziyyat, S., Merten, O.W., Perea, J., and Galy, A. (2011). Quantification of lentiviral vector copy numbers in individual hematopoietic colony-forming cells shows vector dose-dependent effects on the frequency and level of transduction. Gene Ther. *18*, 479–487.

Cong, L., Ran, F.A., Cox, D., Lin, S., Barretto, R., Habib, N., Hsu, P.D., Wu, X., Jiang, W., Marraffini, L.A., and Zhang, F. (2013). Multiplex genome engineering using CRISPR/Cas systems. Science *339*, 819–823.

De Ravin, S.S., Reik, A., Liu, P.Q., Li, L., Wu, X., Su, L., Raley, C., Theobald, N., Choi, U., Song, A.H., et al. (2016). Targeted gene addition in human CD34(+) hematopoietic cells for correction of X-linked chronic granulomatous disease. Nat. Biotechnol. *34*, 424–429.

Dever, D.P., Bak, R.O., Reinisch, A., Camarena, J., Washington, G., Nicolas, C.E., Pavel-Dinu, M., Saxena, N., Wilkens, A.B., Mantri, S., et al. (2016). CRISPR/Cas9 β-globin gene targeting in human haematopoietic stem cells. Nature *539*, 384–389.

Diez, B., Genovese, P., Roman-Rodriguez, F.J., Alvarez, L., Schiroli, G., Ugalde, L., Rodriguez-Perales, S., Sevilla, J., Diaz de Heredia, C., Holmes, M.C., et al. (2017). Therapeutic gene editing in CD34^{+} hematopoietic progenitors from Fanconi anemia patients. EMBO Mol. Med. *9*, 1574–1588.

Du, W., Amarachintha, S., Wilson, A.F., and Pang, Q. (2016). Hyper-active non-homologous end joining selects for synthetic lethality resistant and pathological Fanconi anemia hematopoietic stem and progenitor cells. Sci. Rep. *6*, 22167.

Ebens, C.L., MacMillan, M.L., and Wagner, J.E. (2017). Hematopoietic cell transplantation in Fanconi anemia: current evidence, challenges and recommendations. Expert Rev. Hematol. *10*, 81–97.

Genovese, P., Schiroli, G., Escobar, G., Tomaso, T.D., Firrito, C., Calabria, A., Moi, D., Mazzieri, R., Bonini, C., Holmes, M.C., et al. (2014). Targeted genome editing in human repopulating haematopoietic stem cells. Nature *510*, 235–240.

Gregory, J.J., Jr., Wagner, J.E., Verlander, P.C., Levran, O., Batish, S.D., Eide, C.R., Steffenhagen, A., Hirsch, B., and Auerbach, A.D. (2001). Somatic mosaicism in Fanconi anemia: evidence of genotypic reversion in lymphohematopoietic stem cells. Proc. Natl. Acad. Sci. USA *98*, 2532–2537.

Gross, M., Hanenberg, H., Lobitz, S., Friedl, R., Herterich, S., Dietrich, R., Gruhn, B., Schindler, D., and Hoehn, H. (2002). Reverse mosaicism in Fanconi anemia: natural gene therapy via molecular self-correction. Cytogenet. Genome Res. *98*, 126–135.

Guardiola, P., Socié, G., Li, X., Ribaud, P., Devergie, A., Espérou, H., Richard, P., Traineau, R., Janin, A., and Gluckman, E. (2004). Acute graft-versus-host

disease in patients with Fanconi anemia or acquired aplastic anemia undergoing bone marrow transplantation from HLA-identical sibling donors: risk factors and influence on outcome. Blood *103*, 73–77.

Haeussler, M., Schönig, K., Eckert, H., Eschstruth, A., Mianné, J., Renaud, J.-B., Schneider-Maunoury, S., Shkumatava, A., Teboul, L., Kent, J., et al. (2016). Evaluation of off-target and on-target scoring algorithms and integration into the guide RNA selection tool CRISPOR. Genome Biol. *17*, 148.

Hamanoue, S., Yagasaki, H., Tsuruta, T., Oda, T., Yabe, H., Yabe, M., and Yamashita, T. (2006). Myeloid lineage-selective growth of revertant cells in Fanconi anaemia. Br. J. Haematol. *132*, 630–635.

Heberle, H., Meirelles, G.V., da Silva, F.R., Telles, G.P., and Minghim, R. (2015). InteractiVenn: a web-based tool for the analysis of sets through Venn diagrams. BMC Bioinformatics *16*, 169.

Hoban, M.D., Cost, G.J., Mendel, M.C., Romero, Z., Kaufman, M.L., Joglekar, A.V., Ho, M., Lumaquin, D., Gray, D., Lill, G.R., et al. (2015). Correction of the sickle cell disease mutation in human hematopoietic stem/progenitor cells. Blood *125*, 2597–2604.

Joenje, H., Arwert, F., Eriksson, A.W., de Koning, H., and Oostra, A.B. (1981). Oxygen-dependence of chromosomal aberrations in Fanconi's anaemia. Nature *290*, 142–143.

Kutler, D.I., Auerbach, A.D., Satagopan, J., Giampietro, P.F., Batish, S.D., Huvos, A.G., Goberdhan, A., Shah, J.P., and Singh, B. (2003). High incidence of head and neck squamous cell carcinoma in patients with Fanconi anemia. Arch. Otolaryngol. Head Neck Surg. *129*, 106–112.

Lombardo, A., Genovese, P., Beausejour, C.M., Colleoni, S., Lee, Y.L., Kim, K.A., Ando, D., Urnov, F.D., Galli, C., Gregory, P.D., et al. (2007). Gene editing in human stem cells using zinc finger nucleases and integrase-defective lentiviral vector delivery. Nat. Biotechnol. *25*, 1298–1306.

Mankad, A., Taniguchi, T., Cox, B., Akkari, Y., Rathbun, R.K., Lucas, L., Bagby, G., Olson, S., D'Andrea, A., and Grompe, M. (2006). Natural gene therapy in monozygotic twins with Fanconi anemia. Blood *107*, 3084–3090.

Naka, K., and Hirao, A. (2011). Maintenance of genomic integrity in hematopoietic stem cells. Int. J. Hematol. *93*, 434–439.

Ousterout, D.G., Perez-Pinera, P., Thakore, P.I., Kabadi, A.M., Brown, M.T., Qin, X., Fedrigo, O., Mouly, V., Tremblay, J.P., and Gersbach, C.A. (2013). Reading frame correction by targeted genome editing restores dystrophin expression in cells from Duchenne muscular dystrophy patients. Mol. Ther. *21*, 1718–1726.

Ousterout, D.G., Kabadi, A.M., Thakore, P.I., Majoros, W.H., Reddy, T.E., and Gersbach, C.A. (2015a). Multiplex CRISPR/Cas9-based genome editing for correction of dystrophin mutations that cause Duchenne muscular dystrophy. Nat. Commun. *6*, 6244.

Ousterout, D.G., Kabadi, A.M., Thakore, P.I., Perez-Pinera, P., Brown, M.T., Majoros, W.H., Reddy, T.E., and Gersbach, C.A. (2015b). Correction of dystrophin expression in cells from Duchenne muscular dystrophy patients through genomic excision of exon 51 by zinc finger nucleases. Mol. Ther. *23*, 523–532.

Pace, P., Mosedale, G., Hodskinson, M.R., Rosado, I.V., Sivasubramaniam, M., and Patel, K.J. (2010). Ku70 corrupts DNA repair in the absence of the Fanconi anemia pathway. Science *329*, 219–223.

Pavel-Dinu, M., Wiebking, V., Dejene, B.T., Srifa, W., Mantri, S., Nicolas, C.E., Lee, C., Bao, G., Kildebeck, E.J., Punjya, N., et al. (2019). Gene correction for SCID-X1 in long-term hematopoietic stem cells. Nat. Commun. *10*, 1634.

Pinello, L., Canver, M.C., Hoban, M.D., Orkin, S.H., Kohn, D.B., Bauer, D.E., and Yuan, G.-C. (2016). Analyzing CRISPR genome-editing experiments with CRISPResso. Nat. Biotechnol. *34*, 695–697.

Ran, F.A., Hsu, P.D., Wright, J., Agarwala, V., Scott, D.A., and Zhang, F. (2013). Genome engineering using the CRISPR-Cas9 system. Nat. Protoc. *8*, 2281–2308.

Río, P., Baños, R., Lombardo, A., Quintana-Bustamante, O., Alvarez, L., Garate, Z., Genovese, P., Almarza, E., Valeri, A., Díez, B., et al. (2014). Targeted gene therapy and cell reprogramming in Fanconi anemia. EMBO Mol. Med. *6*, 835–848.

Río, P., Navarro, S., Guenechea, G., Sánchez-Domínguez, R., Lamana, M.L., Yañez, R., Casado, J.A., Mehta, P.A., Pujol, M.R., Surrallés, J., et al. (2017). Engraftment and in vivo proliferation advantage of gene-corrected mobilized $CD34^+$ cells from Fanconi anemia patients. Blood *130*, 1535–1542.

Rodriguez-Perales, S., Torres-Ruiz, R., Suela, J., Acquadro, F., Martin, M.C., Yebra, E., Ramirez, J.C., Alvarez, S., and Cigudosa, J.C. (2016). Truncated RUNX1 protein generated by a novel t(1;21)(p32;q22) chromosomal translocation impairs the proliferation and differentiation of human hematopoietic progenitors. Oncogene *35*, 125–134.

Schiroli, G., Ferrari, S., Conway, A., Jacob, A., Capo, V., Albano, L., Plati, T., Castiello, M.C., Sanvito, F., Gennery, A.R., et al. (2017). Preclinical modeling highlights the therapeutic potential of hematopoietic stem cell gene editing for correction of SCID-X1. Sci. Transl. Med. *9*. Published online October 11, 2017. https://doi.org/10.1126/scitranslmed.aan0820.

Sürün, D., Schwäble, J., Tomasovic, A., Ehling, R., Stein, S., Kurrle, N., von Melchner, H., and Schnütgen, F. (2018). High Efficiency Gene Correction in Hematopoietic Cells by Donor-Template-Free CRISPR/Cas9 Genome Editing. Mol. Ther. Nucleic Acids *10*, 1–8.

Suzuki, K., and Izpisua Belmonte, J.C. (2018). In vivo genome editing via the HITI method as a tool for gene therapy. J. Hum. Genet. *63*, 157–164.

van de Vrugt, H.J., Harmsen, T., Riepsaame, J., Alexantya, G., van Mil, S.E., de Vries, Y., Bin Ali, R., Huijbers, I.J., Dorsman, J.C., Wolthuis, R.M.F., and Te Riele, H. (2019). Effective CRISPR/Cas9-mediated correction of a Fanconi anemia defect by error-prone end joining or templated repair. Sci. Rep. *9*, 768.

Waisfisz, Q., Morgan, N.V., Savino, M., de Winter, J.P., van Berkel, C.G., Hoatlin, M.E., Ianzano, L., Gibson, R.A., Arwert, F., Savoia, A., et al. (1999). Spontaneous functional correction of homozygous fanconi anaemia alleles reveals novel mechanistic basis for reverse mosaicism. Nat. Genet. *22*, 379–383.

Wang, X., Peterson, C.A., Zheng, H., Nairn, R.S., Legerski, R.J., and Li, L. (2001). Involvement of nucleotide excision repair in a recombination-independent and error-prone pathway of DNA interstrand cross-link repair. Mol. Cell. Biol. *21*, 713–720.

Wang, J., Exline, C.M., DeClercq, J.J., Llewellyn, G.N., Hayward, S.B., Li, P.W., Shivak, D.A., Surosky, R.T., Gregory, P.D., Holmes, M.C., and Cannon, P.M. (2015). Homology-driven genome editing in hematopoietic stem and progenitor cells using ZFN mRNA and AAV6 donors. Nat. Biotechnol. *33*, 1256–1263.

Wu, Y., Zeng, J., Roscoe, B.P., Liu, P., Yao, Q., Lazzarotto, C.R., Clement, K., Cole, M.A., Luk, K., Baricordi, C., et al. (2019). Highly efficient therapeutic gene editing of human hematopoietic stem cells. Nat. Med. *25*, 776–783.

STAR★METHODS

KEY RESOURCES TABLE

REAGENT or RESOURCE	SOURCE	IDENTIFIER
Antibodies		
APC/Cyanine7 Anti-human CD45 antibody	BioLegend	Cat# 304014; RRID:AB_314402
APC Mouse Anti-Human CD34 antibody	BD	Cat# 555824
PE Mouse Anti-Human CD33 antibody	Beckman Coulter	Cat# A07775
FITC Mouse Anti-Human CD19 antibody	Beckman Coulter	Cat# IM1284U
PE/Cy7 Anti-human CD3 antibody	BioLegend	Cat# 300420; RRID:AB_10641705
PE Mouse Anti-Human CD8 antibody	Immunotech	Cat# A07757
APC Anti-Human CD4 antibody	Miltenyi Biotech	Cat# 130-091-232; RRID:AB_871690
Rabbit Anti-Human FANCA antibody	Abcam	Cat# ab5063
Mouse Anti-β-actin antibody	Abcam	Cat# ab6276
Mouse Anti-vinculin antibody	Abcam	Cat# ab73412; RRID:AB_1861566
Goat Anti-Rabbit IgG H&L (HRP)	Abcam	Cat# ab6721-1; RRID:AB_955447
Sheep Anti-Mouse IgG H&L (HRP)	Abcam	Cat# ab6808; RRID:AB_955441
Anti-Human FANCD2 antibody	Abcam	Cat# ab2187-50
Goat Anti-Rabbit IgG H&L (Alexa Fluor® 594)	Abcam	Cat# ab150080; RRID:AB_2650602
Bacterial and Virus Strains		
One Shot TOP10 Chemically Competent *E. coli*	ThermoFisher Scientific	Cat# C404003
Biological Samples		
Mobilized peripheral blood hCD34$^+$ cells from patient FA-739	Hospital Niño Jesús	N/A
Mobilized peripheral blood hCD34$^+$ cells from patient FA-807	Hospital Vall d'Hebron	N/A
Mobilized peripheral blood hCD34$^+$ cells from patient FA-655	Hospital Niño Jesús	N/A
Total bone marrow hCD34$^+$ cells from patient FA-807	Hospital Vall d'Hebron	N/A
Chemicals, Peptides, and Recombinant Proteins		
Recombinant Cas9 protein	PNA Bio	Cat# CP02
Human stem cell factor (hSCF)	EuroBiosciences	Cat# rh SCF E.coli
Human FMS-like tyrosine kinase 3 ligand (hFlt3-L)	EuroBiosciences	Cat# rh Flt3L/CD135
Human thrombopoietin (hTPO)	R&D Systems	Cat# 288-TP-200
Human interleukin 3 (hIL3)	Novus Biologicals	Cat# NBP2-34863
Anti-TNFα (Etanercept)	Amgen	Cat# Enbrel
N-acetylcysteine	Pharmazam	
Retronectin®	Takara Bio inc	Cat# T202
Critical Commercial Assays		
NucleoSpin® Gel and PCR Clean-up	Macherey-Nagel	Cat# 740609
HiScribe T7 High Yield RNA Synthesis Kit	New England Biolabs	Cat# E2040S
RNeasy® Plus Mini Kit	QIAGEN	Cat# 74134
SF Cell Line 4D-Nucleofector® X Kit	Lonza	Cat# V4XC-2032
P3 Cell Line 4D-Nucleofector® X Kit	Lonza	Cat# V4XP-3032
DNeasy® Blood & Tissue Kit	QIAGEN	Cat# 69504
Bio-Rad Protein Assay Kit I	BioRad Laboratories	Cat# 5000001
CellROX® Deep Red Reagent	Life Technologies	Cat# C10422
Zero Blunt PCR Cloning Kit	Thermo Fisher Scientific	Cat# K270020
NucleoSpin® Plasmid Kit	Macherey-Nagel	Cat# 740588.250
Deposited Data		
Mendeley Dataset	Mendeley Data	https://doi.org/10.17632/scw4zjsrbv.1

(*Continued on next page*)

Continued

REAGENT or RESOURCE	SOURCE	IDENTIFIER
Experimental Models: Cell Lines		
CP1	Paula Rio	Diez et al., 2017
CP3	Paula Rio	Diez et al., 2017
CP4	Paula Rio	Diez et al., 2017
FA-55	Jordi Surralles' lab	Castella et al., 2011
FA-62	Jordi Surralles' lab	N/A
FA-178	Jordi Surralles' lab	Castella et al., 2011
FA-344	Jordi Surralles' lab	N/A
P2	Helmut Hanenberg's lab	N/A
P3	Helmut Hanenberg's lab	N/A
Experimental Models: Organisms/Strains		
Mouse: Non-obese diabetic (NOD) immunodeficient Cg-Prkdc^{scid} Il2rg^{tm1Wjl}/SzJ (NSG)	The Jackson Laboratory	RRID:IMSR_ARC:NSG
Oligonucleotides		
Oligos for sgRNA cloning in pX330-U6-Chimeric_BB-CBh-hSpCas9 plasmid	See Table S5A	N/A
Primers used for sgRNA *in vitro* transcription	See Table S5B	N/A
Primers used for Sanger sequencing and *ICE* Analyses	See Table S6A	N/A
Primers designed for NGS Analyses	See Table S6B	N/A
Primers for off-target loci NGS Analysis	See Table S7	N/A
Recombinant DNA		
pX330-U6-Chimeric_BB-CBh-hSpCas9	Cong et al., 2013	RRID:Addgene_42230
Software and Algorithms		
CRISPR Design	Zhang Lab	https://zlab.bio/guide-design-resources
CRISPOR	Haeussler et al., 2016;	http://crispor.tefor.net/
Inference of CRISPR editing (ICE)		https://ice.synthego.com/#/
InteractiVenn	Heberle et al., 2015	http://www.interactivenn.net/index2.html#
AxioVision 4.6.3	Carl Zeiss	N/A
Corel Photo-Paint 11	Corel	RRID:SCR_013674
FlowJo Software v7.6.5	FlowJo	RRID:SCR_008520
Finch TV	Digital World Biology LLC	https://digitalworldbiology.com/FinchTV
CRISPResso bioinformatics tool	Pinello et al., 2016	http://crispresso.pinellolab.partners.org/
GraphPad Prism 6.0	Prism	RRID:SCR_002798
Uniprot	Uniprot	https://www.uniprot.org/
Other		
StemMACS HSC-CFU complete with Epo	Miltenyi Biotech	Cat# 130-091-280
Mitomycin C from *Streptomyces caespitosus*	Merk	Cat# M4287-2MG
Complete Mini Protease Inhibitor Cocktail	Merk	Cat# 11836153001
PhosSTOP	Merk	Cat# 4906845001
The Human Gene Mutation Database (HGMD® Professional 2019.1)	Institute of Medical Genetics in Cardiff	http://www.hgmd.cf.ac.uk/ac/index.php

LEAD CONTACT AND MATERIALS AVAILABILITY

Further information and requests for resources and reagents should be directed to and will be fulfilled by the Lead Contact, Dr. Paula Rio (paula.rio@ciemat.es).

EXPERIMENTAL MODEL AND SUBJECT DETAILS

Mice

Non-obese diabetic (NOD) immunodeficient Cg-Prkdc^{scid} Il2rg^{tm1Wjl}/SzJ mice (NSG) used to test the repopulation capacity of hCD34$^+$ cells were purchased from Jackson laboratories. Mice were maintained in pathogen-free conditions and experiments were performed in accordance with the EU and CIEMAT guidelines upon approval of the protocols by the Environment Department in Comunidad de Madrid, Spain (Authorization code PROEX:070/15). At the time of experiments 8-12 age female mice were randomly assigned to the different experimental groups (n = 5 mice per group).

Cell Lines

Lymphoblastic cell lines (LCLs) from healthy donors (HDs) and FA-A patients were generated by transduction of peripheral blood cells with Epstein-Barr virus. Three different HD LCLs were used in this study: CP1, CP3 and CP4; and six FA LCLs: FA-55, FA-62, FA-178, FA-344, P2 and P3 (Table S2). The mutations were confirmed by Sanger sequencing and the characteristic FA mitomycin C (MMC) hypersensitivity checked before starting the experiments. FA patients and HDs were encoded to protect their confidentiality; informed consents were obtained in all cases prior to the generation and use of the cell lines.

LCLs were grown in *Roswell Park Memorial Institute* medium (RPMI, Invitrogen/Life Technologies/Thermo Fisher Scientific), 20% Hyclone, 1% penicillin/streptomycin (P/S) solution (GIBCO/Life Technologies/Thermo Fisher Scientific), 0.005 mM β-mercaptoethanol, 1 mM sodium pyruvate (Sigma) and non-essential aminoacids (Lonza) under normoxic conditions (37°C, 21% O_2, 5% CO_2 and 95% relative humidity -RH-).

Hematopoietic stem and progenitor cells from healthy donors and FA patients

HD hCD34$^+$ cells were obtained from umbilical cord blood (UCB) samples as previously described in Diez et al. 2017 after informed consent was obtained and upon approval by the Centro de Transfusiones de la Comunidad de Madrid.

HSPCs from female and male donors were randomly pooled to obtain enough CD34$^+$ cells. Purities ranging from 85%–98% were routinely obtained. hCD34$^+$ cells were grown in *StemSpam* (StemCell Technologies) supplemented with 1% GlutaMAX (GIBCO), 1% P/S solution (GIBCO), 100 ng/mL human stem cell factor (hSCF, EuroBiosciences), human FMS-like tyrosine kinase 3 ligand (hFlt3-L, EuroBiosciences), human thrombopoietin (hTPO, R&D Systems), and 20 ng/mL human interleukin 3 (hIL3, Novus Biologicals) under normoxic conditions.

A small number of mobilized peripheral blood (mPB) hCD34$^+$ cells from patients FA-739, FA-807 and FA-655 (all males; aged 3-4 years old) that remained in cell collection bags and tubes from the *CliniMACS® System* (Miltenyi Biotec), used for the collection (FANCOSTEM trial; Eudra number CT 2011-006197-88) and the subsequent transduction of hCD34$^+$ cells with LVs (FANCOLEN Trial: Eudra number CT 2011-006100-12) were used after receiving consent from their parents, complying with all relevant ethical regulations and approved by the Ethic Committees at Hospital Vall d'Hebron in Barcelona and Hospital del Niño Jesús in Madrid. Cells were grown in *StemSpam* (StemCell Technologies) supplemented with 1% GlutaMAX (GIBCO), 1% P/S (GIBCO), 100 ng/mL SCF and Flt3, 20 ng/mL TPO and IL3 (all EuroBiosciences), 10 μg/mL anti-TNFα (Enbrel-Etanercept, Pfizer) and 1 mM N-acetylcysteine (Pharmazam) under hypoxic conditions (37°C, 5% of O_2, 5% of CO_2 and 95% RH).

One hCD34$^+$ cell sample from FA-807 patient was also obtained from total bone marrow by immunoselection as indicated for UCB samples and cultured under the same previous conditions.

Since some of the FA samples used were cryopreserved, in all cases 24h of pre-stimulation were used before gene editing.

METHOD DETAILS

Plasmids

Proof-of-concept gene editing experiments in LCLs were performed using the pX330-U6-Chimeric_BB-CBh-hSpCas9 (Cong et al., 2013), which was a gift from Feng Zhang (Addgene plasmid #42230). Guide RNAs to target c.295C > T and c.3558insG mutations were designed using the *CRISPR Design* (http://zlab.bio/guide-design-resources, Zhang Lab) bioinformatics tool from MIT (Table S1).

Guide RNAs were ordered as oligos from Sigma-Aldrich (Table S5A), annealed and cloned into pX330 plasmid after *BbsI* (Ref #R3539, New England Biolabs) restriction enzyme digestion. The obtained plasmids were named as pX330 gGM4, pX330 gGM10, pX330 gINS8 and pX330 gINS11, respectively.

Ribonucleoprotein complex

Gene editing experiments in LCLs and HSPCs were conducted using the ribonucleoprotein complex. Guide RNAs targeting *FANCB*, *FANCC*, *FANCD1* and *FANCD2* mutations were designed using the *CRISPOR* bioinformatic tool (Haeussler et al., 2016) (http://crispor.tefor.net/). Cas9 protein was purchased from PNA Bio (#CP02, PNA Bio), and combined with *in vitro* transcribed (IVT) or chemically modified sgRNAs (MS-sgRNAs) acquired from Synthego for 10 minutes at room temperature (RT).

To generate IVT sgRNAs the T7 promoter sequence was incorporated to the sgRNAs by PCR (Table S5B) using the respective plasmids as PCR templates.

PCR products where purified using the *NucleoSpin® Gel and PCR Clean-up* (Ref 740609, Macherey-Nagel) and directly used for the *in vitro* transcription of the sgRNAs using the *HiScribe T7 High Yield RNA Synthesis Kit* (# E2040S, New England Biolabs) according to manufacturers' instructions. The IVT sgRNAs were purified using *RNeasy® Plus Mini Kit* (Ref 74134, QIAGEN) and quantified using *NanoDrop Spectrophotometer ND-1000* (Thermo Fisher Scientific).

LCLs gene editing

HD and FA patient-derived LCLs were electroporated with 5 μg of pX330 gGM4 / gGM10 / gINS8 / gINS11 plasmid or 9.2 μg of RNP (3.2 μg MS-sgRNA and 6 μg of Cas9) using the *SF Cell Line 4D-Nucleofector® X Kit* for *Amaxa 4-D device* (Lonza). $2x10^5$ cells per condition were electroporated using EW-113 pulse. Cell viability was assessed by flow cytometry 24 hours post-electroporation using 4′, 6-diamidino-2-phenylindole (DAPI).

Gene editing experiments in HD and FA-A HSPCs

HD HSPCs were electroporated with the IVT-RNP complex, composed of 9 μg of Cas9 and 12 μg IVT sgRNA or 6 μg of Cas9 and 3.2 μg MS-sgRNA, using the *P3 Primary Cell 4D-Nucleofector® X Kit* for *Amaxa 4-D device* (Lonza). $2x10^5$ cells per condition were electroporated in separated strip wells using program EO-100 and DZ-100. Cell viability was assessed by flow cytometry 24 hours post-electroporation and gene editing efficacy was evaluated 72 hours post-electroporation by *Inference of CRISPR editing* (*ICE)* and/or next generation sequencing (NGS). Four independent experiments were conducted with MS-sgRNA and 6 with IVT sgRNA. FA HSPCs were electroporated under the same conditions using IVT-RNP complex.

To assess editing efficiencies in the different HSC subpopulations, the electroporated $hCD34^+$ cells were separated by single cell sorting into committed ($hCD34^+$ $hCD133^-$ $hCD90^-$), early ($hCD34^+$ $hCD133^+$ $hCD90^-$) and primitive ($hCD34^+$ $hCD133^+$ $hCD90^+$) HSCs. Three different experiments were conducted.

LCLs single clone isolation

500 cells were plated in methylcellulose to isolate individual clones and incubated under normoxic conditions. Three weeks later Individual colonies were picked and transferred to a 96-well plate for their *in vitro* amplification and characterization.

Colony Forming Unit Assay

900 HD or 10,000 FA-A $hCD34^+$ cells were resuspended in 3 mL of enriched methylcellulose medium (StemMACS HSC-CFU complete with Epo, Miltenyi Biotech). In the case of FA cells, 10 ug/mL anti-TNFα and 1mM N-acetylcysteine were added. Each mL of the triplicate was seeded in a M35 plate and incubated under normoxic (HD $hCD34^+$ cells) or under hypoxic (FA $hCD34^+$ cells) conditions. To test MMC sensitivity in hematopoietic colonies obtained from FA-A patients, 3-10 nM of MMC was added to the culture. Triplicates were conducted with HD $CD34^+$ cells and 2-3 independent plates were plated in FA $hCD34^+$ cells. After fourteen days, colonies were counted using an inverted microscope (Nikon Diaphot, objective 4X) and CFUs-GMs (granulocyte-macrophage colonies) and BFU-Es (erythroid colonies) were identified.

Transplantation of Gene-edited Healthy donor and FA HSPCs in NSG mice

The repopulation capacity of $hCD34^+$ cells was tested by transplantation into non-obese diabetic (NOD) immunodeficient Cg-$Prkdc^{scid}$ $Il2rg^{tm1Wjl}$/SzJ mice (NSG). HD $hCD34^+$ cells from UCB were purified as previously described and electroporated with MS-RNP4 complex using the *P3 Primary Cell 4D-Nucleofector® X Kit* for *Amaxa 4-D device* (Lonza) on the same day. Three groups of cells were established: untreated (control); electroporated cells without nuclease (mock) and electroporated cells with the RNP complex (MS-RNP4). Twenty-four hours later, $3.25x10^5$ cells were transplanted into immunodeficient NSG mice previously irradiated with 1.5 Gy. Five mice were randomly included in each group. Similarly, $1.75x10^5$ $CD34^+$ cells from patient FA-655 were electroporated with IVT-RNP4 and transplanted in an NSG mouse 24h later. One month after transplant BM was obtained and NGS was conducted to study the presence of gene edited cells.

In mouse transplanted with HD $hCD34^+$ cells, human engraftment was measured monthly by flow cytometry analysis of the percentage of $hCD45^+$ cells (anti-hCD45-APC-Cy7, BioLengend). At days 30 and 60 after transplantation bone marrow samples were obtained by intra-bone aspiration. Multi-lineage reconstitution was also evaluated using antibodies against hCD34 (anti-hCD34-APC, BD) for HSPCs, hCD33 (anti-hCD33-Pe, Beckman Coulter) for myeloid cells, hCD19 (anti-hCD19-FITC, Beckman Coulter) for B cells and hCD3 (anti-hCD3-PeCy7, BioLegend) for T cells. The remaining cells were pelleted for DNA extraction and NGS analysis to evaluate the presence of gene edited cells.

At day 90 post-transplantation, mice were euthanized and peripheral blood, spleen, thymus and hind legs were extracted. Bone marrow samples were obtained from hind legs by intra-bone perfusion. Human engraftment was evaluated by flow cytometry according to the percentage of $hCD45^+$ cells in the different hematopoietic organs. Multi-lineage reconstitution was determined using antibodies against hCD34 for HSPCs, hCD33 for myeloid cells, hCD19 for B cells and hCD3 for T cells in peripheral blood, spleen and bone marrow; and using hCD3 for T cells and hCD8 (anti-hCD8-Pe, Immunotech) and hCD4 (anti-hCD4-APC, Miltenyi Biotec) to distinguish between cytotoxic and helper T cells in thymus samples.

To evaluate the long-term engraftment capacity of hCD34$^+$ after NHEJ-mediated gene editing, bone marrow from primary recipients was transplanted into secondary ones mouse to mouse, so the same groups of mice were established. The remaining bone marrow cells were pelleted for DNA extraction using *DNeasy® Blood & Tissue Kit* (QIAGEN) and NGS analysis to evaluate the presence of gene edited cells.

The human engraftment in secondary recipients' follow-up was conducted as previously described: bone marrow aspiration and flow cytometry were performed at 30 and 60 days post-transplantation and hematopoietic organs extraction after euthanasia at day 90 post-transplantation. DNA from bone marrow cells was obtained to evaluate the presence of gene edited cells by NGS at the different time points.

The Venn diagram was generated using the bioinformatic tool *InteractiVenn* (http://www.interactivenn.net/index2.html#) (Heberle et al., 2015).

FANCA protein expression by Western-blot

Protein extracts were isolated from at least 6x10^6 cells in lysis buffer (HEPES 20 mM pH 7.5, NaCl 100 mM, $MgCl_2$ 20 mM, EGTA 10 mM, β-glycerol phosphate 40 mM, 1% de Triton X-100, PMSF 1 mM, protease inhibitors 1X –*Complete Mini Protease Inhibitor Cocktail*, Roche– and phosphatase inhibitors 1X –*PhosSTOP*, Roche–). Cell lysates were centrifuged at 13,000 rpm for 5 minutes at 4°C and supernatants collected. Quantification was conducted by *Bio-Rad Protein Assay Kit* (BioRad Laboratories) according to manufacturer's instructions in a spectrophotometer (Eppendorf BioPhotometer). 50μg of each sample was incubated for 5 minutes at 95°C in redox and denaturing conditions using β-mercaptoethanol and Laemli buffer (BioRad) in a 1:9 ratio. Gel electrophoresis was conducted in 4%–15% polyacrylamide gels (BioRad) using BioRad running buffer (Tris 25 mM, Glycine 192mM, SDS 0.1%; pH 8.3) for 2 hours, following manufacturer's instructions. Proteins were transferred using the *Trans-Blot Turbo Transfer* device from BioRad using BioRad's Transfer Buffer with 10% absolute ethanol. Membranes were blocked for 1 hour at room temperature and agitation with 5% w/v non-fat dry milk in 0.1% Tween-20 PBS. Membrane was stained with rabbit anti-hFANCA antibody (ab5063, Abcam, 1:1,000 dilution in 2.5% milk PBS-T), mouse anti-β-actin antibody (ab6276, Abcam, 1:4,000 dilution in 2.5% milk PBS-T) or mouse anti-vinculin (ab73412, Abcam, 1:500 dilution in 2.5% milk PBS-T) over night at 4°C. β-actin and vinculin served as loading controls. Membrane was washed with PBS buffer three times and then was incubated with 1:5000 dilution in 2.5% milk PBS-T of the secondary anti-rabbit (pAb to Rb IgG-HRP, ab6721-1, Abcam) and anti-mouse (pAb to Ms IgG-HRT ab6808, Abcam) antibodies during 1 hour at RT. Finally, membranes were washed three times with PBS. Blots were visualized with *ChemiDoc MP System*, (BioRad) using *Clarity Western ECL substrate* (BioRad).

Nuclear FANCD2 foci immunofluorescence

One million cells were seeded in chamber slides (Nunc, Sigma) previously coated with 20 μg/cm^2 Retronectin® (Takara Bio inc). Twenty-four hours later cells were incubated in the absence or presence of 40 nM MMC (Sigma) for 16 hours and afterward washed with PBS and fixed with 3.7% paraformaldehyde (Sigma) 15 minutes at room temperature. Then, cells were washed 3 times with TBS (20 mM Tris-HCl; 140 mM NaCl) and permeabilized using 0.5% Triton X-100 (Sigma) for 5 minutes, washed and blocked with blocking solution (0.1% Nonidet-P40 (Sigma); 10% Hyclone) for 4 hours. Cells were incubated with the primary antibody against human FANCD2 (ab2187-50, Abcam) as previously described (Diez et al., 2017), in a humidity chamber at 4°C, overnight, washed 3 times with TBS and then incubated during one hour with the secondary antibody IgG against rabbit, conjugated with AlexaFluor 594 (ab150080, Abcam; 1:1,000 dilution) and DAPI (Roche). Finally, cells were washed 3 times in TBS and slides were mounted with Moviol. Samples were visualized with a fluorescence microscope *Axioplan 2 imaging* (Carl Zeiss) with the objective 0.17 mm and 100x/1.45 magnification. Two hundred cells were counted and cells with more than 10 foci per cell were scored as positive. Each data point represents the mean of at least five independent analyses. Images were captured with *AxioCam MRm* (Carl Zeiss) and processed with *AxioVision 4.6.3* (Carl Zeiss) and *Corel Photo-Paint 11* (Corel).

MMC sensitivity test

2.5x10^5 cells were exposed to increasing concentrations of MMC (from 0 to 1,000 nM). Cell viability was measured 5 to 15 days after MMC treatment by flow cytometry using DAPI vital marker in a *LSRFortessa Cell Analyzer*. Offline analysis was performed with *FlowJo Software v7.6.5*. Each data point represents the mean of at least three independent analyses.

Chromosome Diepoxybutane Analysis

Cytogenetic analysis was performed on metaphase spreads obtained from cell culture, as previously described (Rodriguez-Perales et al., 2016). Briefly, cells were cultured in RPMI 1640 containing 10% fetal calf serum (FCS), 1% antibiotics and 1% L-glutamine at 37°C in an atmosphere of 5% CO2. DEB, a highly reactive DNA cross-linking agent, was added to the cultures at a final concentration of 0.1 μg/mL (Sigma). Cultures were paired for DEB studies, with a replicate set of cultures to serve as untreated controls. After 48 hours of DEB treatment, cells were induced to mitotic arrest with 0.1 μg/mL Colcemid (GIBCO). Metaphases were prepared by standard cytogenetic methods including hypotonic treatment (75 mm KCl) and fixation with methanol/acetic acid (3:1) before spreading onto slides. At least 100 metaphases were blindly analyzed by microscopic analysis (Leica) for each culture after standard Giemsa staining.

Chromosome fragility by the flow cytometric micronucleus test

Cells were processed by flow cytometry following the procedure previously described (Avlasevich et al., 2006). One million lymphoblastic cells were untreated or treated with 0.1 μg/mL of DEB and maintained in culture for at least one population doubling. Cells were then sequentially stained; first with ethidium monoazyde bromide (EMA) (0.025 mg/mL) and second with Sytox green (0.2 μM). Next, a lysis step with 250 μL of lysis solution 1 (0.584 mg/mL NaCl, 1 mg/mL sodium citrate, 0.3 μg/mL IGEPAL, 1 mg/mL RNase A and 0.2 μM Sytox green in deionized water) for 1 h at RT was conducted, followed by a second lysis step using 250 μL of solution lysis 2 (85.6 mg/mL sucrose, 15 mg/mL citric acid and 0.2 μM Sytox green in deionized water) for 30 min at RT. After lysis, samples were stored at 4°C until being processed by flow cytometry. Data acquisition was performed by flow cytometry with FACSCalibur. Collected data was analyzed by *FlowJo Software v7.6.5*. The data of micronuclei (MN) presented in this work represents results from three independent analyses each one conducted in duplicate.

Analysis of reactive oxygen species (ROS)

Detection of intracellular Reactive Oxygen Species (ROS) was conducted using the *CellROX® Deep Red Reagent* (C10422, Life Technologies). *The CellROX® Deep Red dye* is a fluorogenic compound that enters the cells in a reduced state as a non-fluorescent probe exhibiting strong fluorogenic signal (640nm excitation and 665 nm emission) after oxidation by the presence of reactive oxygen species. The analysis was performed in FA-A patient LCLs (gene-edited and untreated) following manufacturer's instructions: $5x10^4$ cells were incubated with *CellROX® Deep Red Reagent* at a final concentration of 5 μM in PBS during 20 min at 37°C. After incubation, cells were washed with PBA and DAPI (Roche) was added. Quantification of ROS production was conducted in *LSRFortessa Cell Analyzer* and data were analyzed with *FlowJo Software v7.6.5*. A Z-score was conducted. Each data point represents the mean of 3 independent analyses.

NHEJ-repair events characterization by Sanger Sequencing

DNA obtained from the isolated gene edited LCL clones and the CFCs from HD/FA HSPCs was used as a template to amplify by PCR the CRISPR/Cas9 target sites using *Herculase II fusion DNA polymerase* (Agilent). PCR products were cloned using *Zero Blunt PCR Cloning Kit* (Thermo Fisher Scientific) and plasmids transfected into TOP10 competent cells by heat-shock. The transformation was plated in selective Luria-Bertani medium (Sigma) plates and incubated overnight at 37°C. At least 3 individual colonies were picked to obtain products coming from both alleles and grown overnight in selective LB medium in a shaker at 37°C. Plasmids were extracted using *NucleoSpin® Plasmid Kit* (Macherey-Nagel) and sent to Stabvida to conduct Sanger sequencing using M13 primers. Chromatograms were visualized using Finch TV (Digital World Biology LLC).

CRISPR/Cas9-induced gene editing analysis by Inference of CRISPR Editing (ICE)

DNA isolated from edited and control LCLs or primary cells was sequenced by Sanger and chromatograms were analyzed by *ICE* (https://ice.synthego.com/#/). Percentage of editing was calculated according to the frameshift produced in the edited chromatogram compared to the control sequence and the most probable indels can also be inferred. Primers used in these PCRs are listed in Table S6A.

CRISPR/Cas9-induced gene editing analysis by Next Generation Sequencing

NGS analyses from LCLs samples were conducted by *StabVida* while those corresponding to HSPCs were conducted by *Genewiz*.

Genomic DNA from edited LCLs or $hCD34^+$ cells was extracted using the *NucleoSpin Tissue kit* (Macherey-Nagel) or the *Proteinase K Lysis protocol* (Charrier et al., 2011). Target sites were amplified by PCR, generating amplicons of 200 bp surrounding the potential CRISPR binding site. Primers used in these PCRs are listed in Table S6B. PCR products were purified using the AxyPrep PCR Clean-Up (Axygen), quantified using a *Qubit fluorometer* (Thermo Fisher Scientific), and used for library construction with the *KAPA Library preparation Kit* (Kapa Biosystems) for Illumina platforms. The generated DNA fragments (DNA libraries) were sequenced with v3 chemistry in the *Illumina MiSeq platform*, using 250-bp paired-end sequencing reads.

The analysis of the raw sequence data obtained was carried out using *CLC Genomics Workbench 9.5.4* and those high-quality sequencing reads were mapped against the reference sequences using a length and a similarity fraction of 0.80. A low frequency variant calling was performed, obtaining a list of variants with a low representation within each sample following two criteria: a minimum frequency of 0.01% (and a probability of 0.0001); and a forward/reverse sequence read balancement $\geq$ 30% combined with localization in homopolymeric regions $\leq$ 2 nucleotides. Those sequences containing indels of $\geq$ 1 bp located within a region encompassing ± 5 bp from the cleavage site were considered as CRISPR-induced genome modifications. The frequency of each indel was calculated by relativizing the number of times that was detected to the total number of reads.

Next Generation Sequencing analysis of putative off-targets

The most probable gGM4 off target loci were predicted *in silico* using the CRISPR Design web tool from MIT. Among the different off-targets that were identified, we studied the top five and top twenty in FA and HD HSPCs respectively.

Genomic DNA from FA patient $hCD34^+$ cells targeted using RNP4 complex 5 days after electroporation was extracted using the *NucleoSpin Tissue Kit* (Macherey-Nagel) or the *Proteinase K Lysis protocol* (Charrier et al., 2011). The putative off-target sites were amplified by PCR including Illumina adapters in the primer sequence, generating amplicons of 200 bp surrounding the potential CRISPR binding site. Primers used in these PCRs are listed in Table S7. The following procedure was conducted by Servicio

de Genómica y Bioinformática from Universidad Autónoma de Barcelona. PCR products were purified using the *AxyPrep PCR Clean-Up* (Axygen), quantified by *Qubit fluorometer* (Thermo Fisher Scientific), and used for library construction using the *KAPA Library preparation Kit* (Kapa Biosystems) for Illumina platforms. The generated DNA fragments (DNA libraries) were sequenced on *MySeq platform*, using 150-bp paired-end sequencing reads. The raw data results were analyzed and interpreted using the *CRISPResso* bioinformatics tool (Pinello et al., 2016) (http://crispresso.rocks/). Those sequences containing indels of $\geq$ 1 bp located within a region encompassing ± 5 bp from the cleavage site were considered as CRISPR-induced genome modifications.

Potential mutations to be treated by NHEJ-mediated gene editing

The identification of mutations in different blood disorders that could be potentially corrected by NHEJ-based gene editing strategy was conducted using The Human Gene Mutation Database (HGMD® Professional 2019.1) at the Institute of Medical Genetics in Cardiff (http://www.hgmd.cf.ac.uk/ac/index.php). For this analysis, nonsense mutations, small insertions and deletions were considered.

QUANTIFICATION AND STATISTICAL ANALYSIS

The statistical analysis was performed using *GraphPad Prism* software package for Windows (version 6.0, GraphPad Software). For the analyses of experiments in which $n < 5$, a nonparametric two-tailed Mann–Whitney test was performed when two variables were compared, or Kruskal-Wallis with Dunn's multiple comparison test when more than two variables were compared. In the experiments in which $n \geq 5$, a Kolmogorov-Smirnov test was done to test the normal distribution of the samples. If samples showed a normal distribution, a parametric two-tailed paired t test was performed when two variables were compared or an ANOVA with Tukey's multiple comparisons test when more than two variables were compared. If samples did not follow normal distribution, the previously mentioned nonparametric tests were used. All the statistical details of the experiments conducted in this study can be found in the corresponding figures and legends.

DATA AND CODE AVAILABILITY

Main Source Data have been deposited in the Mendeley database under DOI: https://doi.org/10.17632/scw4zjsrbv.1. All other data are available from the Lead Contact upon request.

Cell Stem Cell, Volume *25*

Supplemental Information

NHEJ-Mediated Repair of CRISPR-Cas9-Induced DNA Breaks Efficiently Corrects Mutations in HSPCs from Patients with Fanconi Anemia

Francisco José Román-Rodríguez, Laura Ugalde, Lara Álvarez, Begoña Díez, María José Ramírez, Cristina Risueño, Marta Cortón, Massimo Bogliolo, Sara Bernal, Francesca March, Carmen Ayuso, Helmut Hanenberg, Julián Sevilla, Sandra Rodríguez-Perales, Raúl Torres-Ruiz, Jordi Surrallés, Juan Antonio Bueren, and Paula Río

SUPPLEMENTAL TABLES

Table S1. Designed sgRNAs used in this study, Related to STAR Methods.

Gene	Target mutation	sgRNA name	Sequence (5' to 3')	Orientation
FANCA	c.3558insG	gINS8	CTCCACCGGCAGAGCAGCAC	Antisense
		gINS11	ACTGCCAGAGCCCGCTGCCC	Sense
	c.295C>T	gGM4	CACGGGAACCCCCAGCCTTG	Antisense
		gGM10	AGGATCAAGCCTCAAGGCTG	Sense
		gGM0	TGTTTAAGGCTCTGCTTTGT	Sense
FANCB	c.1815_1816delAA	gP2	TACAAATTATGGAGAGAGAG	Sense
FANCC	c.67delC	gP3	AGAAGCTTTCTGTATGGATC	Sense
FANCD1/BRCA2	c.1596delA	gFA62	TATTTCCAGTCCACTTTCAG	Antisense
FANCD2	c.718delT	gFA344	AGTGAGTATTCTCTATCAGT	Antisense

Table S2. FA lymphoblastic cell lines (LCLs) used in this study, Related to STAR Methods.

Gene	LCL	Target mutation	Genotype
FANCA	FA-178	c.3558insG	Homozygous
	FA-55	c.295C>T	Homozygous
FANCB	P2	c.1815_1816delAA	Homozygous
FANCC	P3	c.67delC	Homozygous
FANCD2	FA-344	c.718delT	Heterozygous (c.3707 G>A)
FANCD1/BRCA2	FA-62	c.1596delA	Heterozygous (ex15-16del)

Table S3. Editing events described in Venn Diagram, Related to Figure 5D.

Code	Indels
A	c.311delG
	c.304_311del8
	c.306_312del7
	c.312_314del3
	c.311insG
B	c.310insA
	c.311_316del6
	c.309delA
C	c.311_314del4
D	c.296_309del14
E	c.311_313del3
	c.290_310del21
	c.296_310del15
	c.294_311del18
	c.297_317del21
	c.309_311del3
	c.312_323del12
F	c.311_312del2
	c.300_306del7
G	c.311_315del5
H	c.310insAA
	c.312ins3
	c.311_319del9
	c.293_325del33
I	c.300_320del21
	c.310_312del3
	c.307_311del5
J	c.308delC, c.309A>T
	c.311_324del14
	c.307delT, c.310_312del3
	c.299_310del12
	c.305_310del6
K	c.312insT
	c.311_318del8
	c.311_317del7
L	c.312_313del2
M	c.311insT

Code	Indels
N	c.307_309del3, c.310A>C
	c.307_309del3
	c.289_318del30
O	c.293_310del18
	c.292_315del24
	c.308ins3
	c.311G>A, c.314ins3, c.314T>A, c.315G>A, c.316G>A
	c.312ins5
P	c.310_317del8
	c.304_317del14
	c.292_323del32
	c.308_310del3
Q	c.307T>C, c.309_311del3
	c.293_319del27
	c.315delG
R	c.307_320del14
	c.305_321del17
	c.312insGG
	c.309_310del2
	c.306_310del5
	c.306_335del30

Code	Indels
S	c.311delG, c.308C>T
	c.299_302del4, c.309ins6, c.310_317del8
	c.306_326del21
	c.313ins2, c.314_321del8
	c.300_312del13
	c.308_324del17
	c.296_311del16
	c.304_319del16
	c.309_320del12
	c.313ins2
	c.297_316del20
	c.311G>A
	c.312_314del3, c.315T>G
	c.301_315del15
	c.289_317del29
	c.313ins23
	c.298_310del13
	c.311delG, c.312G>A
	c.284-1_317del35
	c.311G>A, c.312G>C, c.313insA
	c.303_330del28
	c.311delG, c.313C>T
	c.312_320del9
	c.312ins2, c.316ins7
	c.312insC, c.315_316del2
	c.311_312del2, C.316delG
	c.307_319del13
	c.309delA, c.310A>G
	c.307_318del12
	c.314_328del15
	c.313ins6
	c.310_325del16
	c.298_320del23
	c.307T>C, c.310_312del3

Code	Indels
T	c.300_325del26
	c.310_311del2
	c.308ins9
	c.297_314del18
	c.308ins23
	c.284-1_322del40
	c.311ins2
	c.309_314del6
	c.302_310del9
	c.307_317del11
	c.293_315del23
	c.297_311del15
	c.293_313del21
	c.312insG
	c.301_323del23
	c.286_310del35
	c.295_321del27
	c.311ins4
	c.284-4_308del28
	c.300_314del15
	c.293_308del16, c.311_315del5
	c.313ins39
U	c.309_311del3, c.316delG
	c.309A>G, c.311insG
	c.315C>T
	c.312insC
	c.284-1_24del42
	c.312insA
	c.284-14ins35, c.304G>C, c.307_312del5, c.313GZA
	c.295_322del28
	c.311G>T,312G>A,313insC
	c.299_308del8
	c.311ins9
	c.295_309del15
	c.307_310del4, c.311G>C

V	c.308C>T, c.311_313del3
	c.311_313del3, c.314T>C
	c.310A>T
	c.308C>T
	c.308C>G
	c.306_333del28
	c.284-9_318del44
	c.313insG, c.316G>A
	c.300_334del35
	c.311_313del3, c.315G>A
	c.303_308del6
	c.311insA
	c.311ins3
	c.309delA, c.310A>C
	c.309_312del3, c.316delG
	c.310delA
	c.313C>G, c.314insT
	c.313insA
	c.297_323del27
	c.309_311del3, c.313C>A
	c.312G>A
	c.307_329del23
	c.315G>A
	c.31_316del6
	c.311insAA c.310_318del9
	c.314T>A
	c.307T>C, c.313insG
	c.312G>C, c.313C>T, c.314T>G
	c.309A>G, c.313insG
	c.311ins37
	c.307T>G
	c.307T>A, c,308C>A, c.309A>G, c.310A>C, c.311ins3
	c.284-3_308del28
	c.308_310del3, c.311G>A
	c.301_310del10
	c.310_312del3, c.313C>G
	c.309A>G
	c.313insG, c.315T>C
	c.316G>T
	c.311G>A, c.313ins3, c.314T>A, c.315G>A, c.316G>A

Table S4. Diseases susceptible to be treated by NHEJ-based gene editing, Related to Figure 3.

Recessive or X linked blood disorders	Gene	Nonsense (*)	Small deletions	Small insertions	Small indels	Total targetable mutations	Total mutations described	Mutations targetable by NHEJ (%)
X1-SCID	*IL2RG*	44	49	16	7	116	256	45.3
Adenosin deaminase deficiency	*ADA*	8	11	2	2	23	96	24.0
β-thalassemia	*HBB*	23	133	48	22	226	884	25.6
Wiskot-Aldrich syndrome	*WAS*	45	132	52	7	236	443	53.3
Chronic granulomatous disease	*CYBB*	106	160	57	29	352	790	44.6
Fanconi anemia complementation group A	*FANCA*	78	98	43	4	223	693	32.2
Fanconi anemia complementation group B	*FANCB*	5	5	1	0	11	22	50.0
Fanconi anemia complementation group C	*FANCC*	12	12	6	2	32	66	48.5
Fanconi anemia complementation group D2	*FANCD2*	7	9	2	2	20	65	30.8
Fanconi anemia complementation group E	*FANCE*	3	3	2	0	8	18	44.4
Fanconi anemia complementation group F	*FANCF*	4	5	0	0	9	16	56.3
Fanconi anemia complementation group G	*FANCG*	15	25	12	4	56	92	60.9
Fanconi anemia complementation group I	*FANCI*	9	11	2	0	22	45	48.9
Shwachman diamond syndrome	*SBDS*	4	9	1	5	19	90	21.1
Severe congenital neutropenia	*HAX1*	4	4	5	0	13	21	61.9
Dyskeratosis congenita	*DKC1*	0	4	1	4	9	75	12.0
Bernard Soulier Syndrome type A	*GP1BA*	13	16	11	1	41	78	52.6
Bernard Soulier Syndrome type B	*GP1BB*	6	5	3	1	15	53	28.3
Bernard Soulier Syndrome type C	*GP9*	4	3	1	0	8	42	19.0
Hemophilia A	*F8*	327	539	189	42	1097	3246	33.8
Hemophilia B	*F9*	100	174	59	19	352	1288	27.3
Leucocyte adhesion deficiency type 1	*ITGB2*	18	17	5	3	43	119	36.1
Diamond-Blackfan Anemia	*RPS19*	15	38	27	3	83	175	47.4
Diamond-Blackfan Anemia	*RPS26*	1	6	3	0	10	34	29.4
Diamond-Blackfan Anemia	*RPS24*	2	2	0	1	5	10	50.0
Diamond-Blackfan Anemia	*RPS17*	1	3	0	1	5	19	26.3

Diamond-Blackfan Anemia	*RPL5*	19	27	16	4	66	98	67.3
Diamond-Blackfan Anemia	*RPL11*	5	19	12	1	37	56	66.1
Diamond-Blackfan Anemia	*RPL35A*	1	2	0	0	3	19	15.8
Diamond-Blackfan Anemia	*RPL15*	3	0	1	0	4	9	44.4
Diamond-Blackfan Anemia	*GATA1*	0	1	0	1	2	16	12.5
Diamond-Blackfan Anemia	*RPS10*	1	0	4	0	5	7	71.4
Diamond-Blackfan Anemia	*RPS7*	0	1	0	0	1	10	10.0
								Mean: 39.3

* Estimated value considering that missense and nonsense are shown together in HGMD database.

FA genes involved in cancer have not been included since many of the mutations described in the data base are not associated to FA.

Diamond-Blackfan anemia: the most frequently described genes associated to the disease have been included.

Table S5. Primers used for sgRNA cloning in pX330-U6-Chimeric_BB-CBh-hSpCas9 plasmid (A) and for sgRNA *in vitro* transcription (B), Related to STAR Methods.

gRNA	Primer	Sequence (5' to 3')
A. Primers used for sgRNA cloning in pX330-U6-Chimeric_BB-CBh-hSpCas9 plasmid		
gINS8	Fw	CACCGCTCCACCGGCAGAGCAGCAC
	Rv	AAACGTGCTGCTCTGCCGGTGGAGC
gINS11	Fw	CACCGACTGCCAGAGCCCGCTGCCC
	Rv	AAACGGGCAGCGGGCTCTGGCAGTC
gGM4	Fw	CACCGCACGGGAACCCCCAGCCTTG
	Rv	AAACCAAGGCTGGGGGTTCCCGTGC
gGM10	Fw	CACCGAGGATCAAGCCTCAAGGCTG
	Rv	AAACCAGCCTTGAGGCTTGATCCTC
B. Primers used for sgRNA *in vitro* transcription		
gINS11	Fw	GAAATTAATACGACTCACTATAGACTGCCAGAGCCCGCTGCCC
	Rv	AAAAGCACCGACTCGGTGCC
gGM4	Fw	GAAATTAATACGACTCACTATAGCACGGGAACCCCCAGCCTTG
	Rv	AAAAGCACCGACTCGGTGCC

Table S6. Primers used for Sanger sequencing and *ICE* analyses (A) and for NGS analyses (B), Related to STAR Methods.

Gene	Mutation	Primer	Sequence (5' to 3')	Tm (°C)	PCR product size (bp)
A. Primers used for Sanger sequencing and ICE analyses					
FANCA	c.3558insG	Fw	TGTAGTGGCCTGTAGGAGCA	60	394
		Rv	CCCAGTAGTTGGGATTACAG		
	c.295C>T	Fw	TGCTCCTTTTGTGTCATGGGA	60	422
		Rv	TGCTGGTGTCTTACTCTCTGC		
FANCB	c.1815_1816delAA	Fw	ACGTTGACCCCTGATAGCAA	60	236
		Rv	ACTTCCCAGTTGAAAGATCTTCT		
FANCC	c.67delC	Fw	GGGACATCACCTTTTCGCTT	60	194
		Rv	ACCATCTCTTTCAAGGCTTCA		
FANCD1/ BRCA2	c.1596delA	Fw	AGTGGCTTCTTCATTTCAGGGT	60	232
		Rv	AATTCTGTGTGGTGGTGGCT		
FANCD2	c.718delT	Fw	CTGCCCAGCTCTGTTCAAAC	60	226
		Rv	ACTCCCAAGGCAATGACTGA		
B. Primers used for NSG analyses					
FANCA	c.3558insG	Fw	**ATCTCAGCCACCCTCATCTG**	60	176
		Rv	**ATCTCACCACCCACACGTAC**		
	c.295C>T	Fw-StV	**CCTTTGCATCTATTCTCCCCGT**	60	234
		Rv-StV	**TGCAGATCTGTCCCACGCTA**		
		Fw-Gwz	ACACTCTTTCCCTACACGACGCTCTTCCGATCT**CCTTTGCATCTATTCTCCCCGT**	60	299
		Rv-Gwz	GACTGGAGTTCAGACGTGTGCTCTTCCGATCT**TGCAGATCTGTCCCACGCTA**		
		Fw-UAB	TCGTCGGCAGCGTCAGATGTGTATAAGAGACAG**CCTTTGCATCTATTCTCCCCGT**	60	301
		Rv-UAB	GTCTCGTGGGCTCGGAGATGTGTATAAGAGACAG**TGCAGATCTGTCCCACGCTA**		
FANCB	c.1815_1816delAA	Fw	ACACTCTTTCCCTACACGACGCTCTTCCGATCT**ACGTTGACCCCTGATAGCAA**	60	301
		Rv	GACTGGAGTTCAGACGTGTGCTCTTCCGATCT**ACTTCCCAGTTGAAAGATCTTCT**		
FANCC	c.67delC	Fw	ACACTCTTTCCCTACACGACGCTCTTCCGATCT**GGGACATCACCTTTTCGCTT**	60	259
		Rv	GACTGGAGTTCAGACGTGTGCTCTTCCGATCT**ACCATCTCTTTCAAGGCTTCA**		
FANCD1/ BRCA2	c.1596delA	Fw	ACACTCTTTCCCTACACGACGCTCTTCCGATCT**AGTGGCTTCTTCATTTCAGGGT**	60	297
		Rv	GACTGGAGTTCAGACGTGTGCTCTTCCGATCT**AATTCTGTGTGGTGGTGGCT**		
FANCD2	c.718delT	Fw	ACACTCTTTCCCTACACGACGCTCTTCCGATCT**CTGCCCAGCTCTGTTCAAAC**	60	291
		Rv	GACTGGAGTTCAGACGTGTGCTCTTCCGATCT**ACTCCCAAGGCAATGACTGA**		

Adapter sequences are indicated in regular letters, while primer sequences are marked in bold.

Table S7. Primers for off-target loci NGS Analysis, Related to STAR Methods.

Off-target	Primer	Sequence (5' to 3')	Tm (°C)	PCR size (bp)
OT1	Fw	TCGTCGGCAGCGTCAGATGTGTATAAGAGACAG**GCAAGTGGGAAAACACAGGT**	62	299
	Rv	GTCTCGTGGGCTCGGAGATGTGTATAAGAGACAG**AGACCCCTCTTCAGGAAGTC**		
OT2	Fw	TCGTCGGCAGCGTCAGATGTGTATAAGAGACAG**TCCAGGGCTGGAATGTAGTC**	62	260
	Rv	GTCTCGTGGGCTCGGAGATGTGTATAAGAGACAG**GCTTCTGAGCTGCAAGGTCT**		
OT3	Fw	TCGTCGGCAGCGTCAGATGTGTATAAGAGACAG**AGTGCCACCAGAGGTTAGGT**	62	228
	Rv	GTCTCGTGGGCTCGGAGATGTGTATAAGAGACAG**CTCACCCTCCATATGGGACA**		
OT4	Fw	TCGTCGGCAGCGTCAGATGTGTATAAGAGACAG**CGCTTCCTGACATGATGGT**	62	235
	Rv	GTCTCGTGGGCTCGGAGATGTGTATAAGAGACAG**AGGCACAGGTGCTTTACCTC**		
OT5	Fw	TCGTCGGCAGCGTCAGATGTGTATAAGAGACAG**GGGAACAGCCAGTTCTCATC**	62	250
	Rv	GTCTCGTGGGCTCGGAGATGTGTATAAGAGACAG**TGCATGTGGAGGTGGTACAT**		
OT6	Fw	TCGTCGGCAGCGTCAGATGTGTATAAGAGACAG**CATTCCCTTGGGAAATCCTT**	60	259
	Rv	GTCTCGTGGGCTCGGAGATGTGTATAAGAGACAG**AAAGCCCCTGTGTAGGGAAG**		
OT7	Fw	TCGTCGGCAGCGTCAGATGTGTATAAGAGACAG**GGGCTCTGTGTGCTAAAGGA**	60	279
	Rv	GTCTCGTGGGCTCGGAGATGTGTATAAGAGACAG**AGAAACTGCCTGGAGCTGAG**		
OT8	Fw	TCGTCGGCAGCGTCAGATGTGTATAAGAGACAG**CAAGTGCCCTCTTGGACTTC**	60	245
	Rv	GTCTCGTGGGCTCGGAGATGTGTATAAGAGACAG**GAAGCATGGAGCCCATAGTC**		
OT9	Fw	TCGTCGGCAGCGTCAGATGTGTATAAGAGACAG**CAGCAGAGACCATTAGCCTTC**	64	310
	Rv	GTCTCGTGGGCTCGGAGATGTGTATAAGAGACAG**CGTTTCAGATGCCATGACTG**		
OT10	Fw	TCGTCGGCAGCGTCAGATGTGTATAAGAGACAG**TAAGGAAGAGCAGGGCACTC**	60	273
	Rv	GTCTCGTGGGCTCGGAGATGTGTATAAGAGACAG**AGAGGGCATAAAGGGACCTC**		
OT11	Fw	TCGTCGGCAGCGTCAGATGTGTATAAGAGACAG**CCCCAAGCTAGCAACACAAT**	60	245
	Rv	GTCTCGTGGGCTCGGAGATGTGTATAAGAGACAG**CAGAGTTGTTGGCTCCTGTG**		
OT12	Fw	TCGTCGGCAGCGTCAGATGTGTATAAGAGACAG**TTGATGCCTGCAAGTCTCTG**	64	316
	Rv	GTCTCGTGGGCTCGGAGATGTGTATAAGAGACAG**CTGGGTTGGGTTATCACTGG**		
OT13	Fw	TCGTCGGCAGCGTCAGATGTGTATAAGAGACAG**AAGCCACTGTCCCTCTCCTT**	60	245
	Rv	GTCTCGTGGGCTCGGAGATGTGTATAAGAGACAG**CACAAATGCCGCTGATGTC**		
OT14	Fw	TCGTCGGCAGCGTCAGATGTGTATAAGAGACAG**TGAGCTTCACCTTGTGGTTG**	56	295
	Rv	GTCTCGTGGGCTCGGAGATGTGTATAAGAGACAG**CCAGAAGCAGGTCATGTTGA**		
OT15	Fw	TCGTCGGCAGCGTCAGATGTGTATAAGAGACAG**CCTCAGCTGCCACTGTGATA**	64	242
	Rv	GTCTCGTGGGCTCGGAGATGTGTATAAGAGACAG**TGGGGCATCATCTCCTAAAG**		
OT16	Fw	TCGTCGGCAGCGTCAGATGTGTATAAGAGACAG**TGTACGTGCAGCCAAGAAAG**	64	252
	Rv	GTCTCGTGGGCTCGGAGATGTGTATAAGAGACAG**GAAGGGCATGTGTCCTGAAT**		
OT17	Fw	TCGTCGGCAGCGTCAGATGTGTATAAGAGACAG**CAGTGTGGCATGTCAAATCC**	64	300
	Rv	GTCTCGTGGGCTCGGAGATGTGTATAAGAGACAG**GTCCATGGAGAAATGGAAGC**		
OT18	Fw	TCGTCGGCAGCGTCAGATGTGTATAAGAGACAG**ATTTCCTCGGTTTCTGAGCA**	60	226
	Rv	GTCTCGTGGGCTCGGAGATGTGTATAAGAGACAG**AGGAAACTCTTCCCGAGTCC**		
OT19	Fw	TCGTCGGCAGCGTCAGATGTGTATAAGAGACAG**CCACATCACCAAACTGACCA**	64	222
	Rv	GTCTCGTGGGCTCGGAGATGTGTATAAGAGACAG**CGTTAAGCTTTGCCCTTCAG**		
OT20	Fw	TCGTCGGCAGCGTCAGATGTGTATAAGAGACAG**AGAGGGAGAGTGAAGGCTGA**	64	306
	Rv	GTCTCGTGGGCTCGGAGATGTGTATAAGAGACAG**GACACTACGTGGGGAAATGG**		

Adapter sequences are indicated in regular letters, while primers sequences are marked in bold.

SUPPLEMENTAL FIGURES

Figure S1

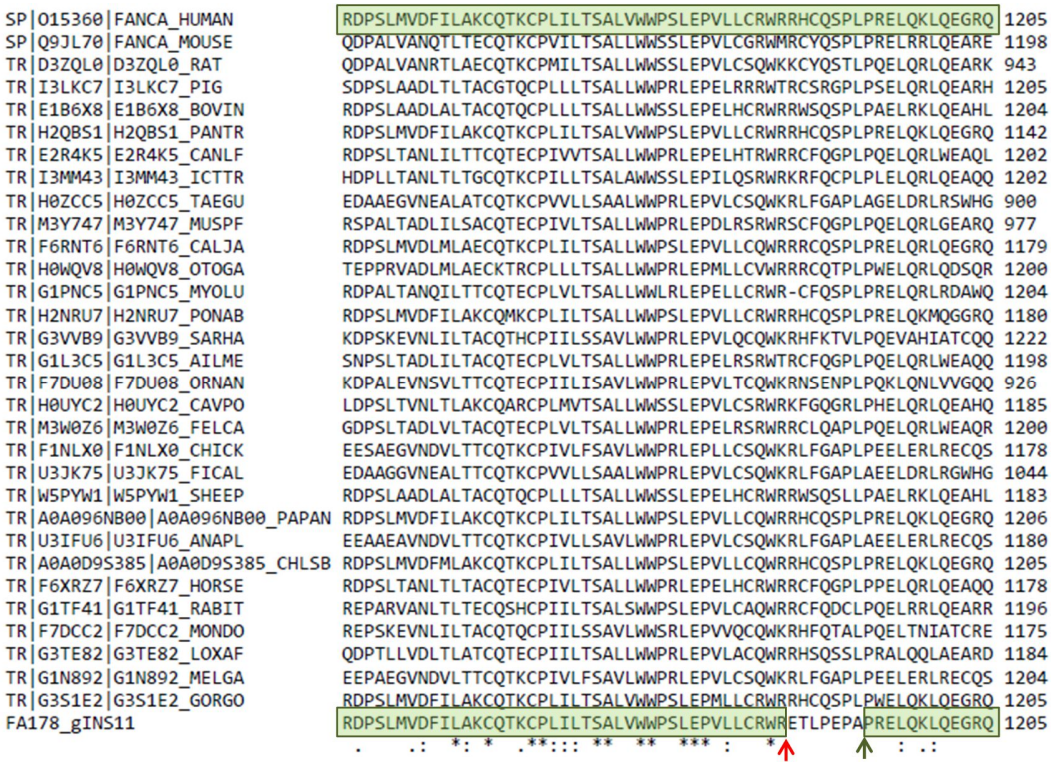

Figure S1. FANCA protein BLAST analysis suggests that exon 36 is a highly conserved domain, Related to Figure 1. A protein BLAST analysis was conducted using the bioinformatic tool available in the Uniprot webpage (https://www.uniprot.org/). The FANCA protein amino acid sequences available of FANCA proteins from different vertebrates were compared in order to identify the most conserved regions. The results obtained evidenced that exon 36 sequence is one of the most conserved, which implies that very few variations could be admitted without compromising the functionality of the protein. This fact perfectly explains why the deletion of the G next to the Cas9 cutting site is the only event that became more frequent over time among the wide variations of corrective NHEJ-repair events obtained in gene edited FA-178 LCL, as the sequence comprised between the c.3558insG mutation (where the frameshift starts –red arrow–) and the c.3579delG generated by NHEJ after the DSB (where the ORF is restored –green arrow–) is not conserved. Conversely, as the other potentially corrective indels implied higher deletions, a conserved domain was affected and the functionality of the protein was impaired. According to Uniprot protein BLAST analysis tool: "*****" (asterisk) indicates positions which have a single, fully conserved residue; "**:**" (colon) indicates conservation between groups of strongly similar properties - scoring > 0.5 in the Gonnet PAM 250 matrix and "**.**" (period) indicates conservation between groups of weakly similar properties - scoring =< 0.5 in the Gonnet PAM 250 matrix.

Figure S2

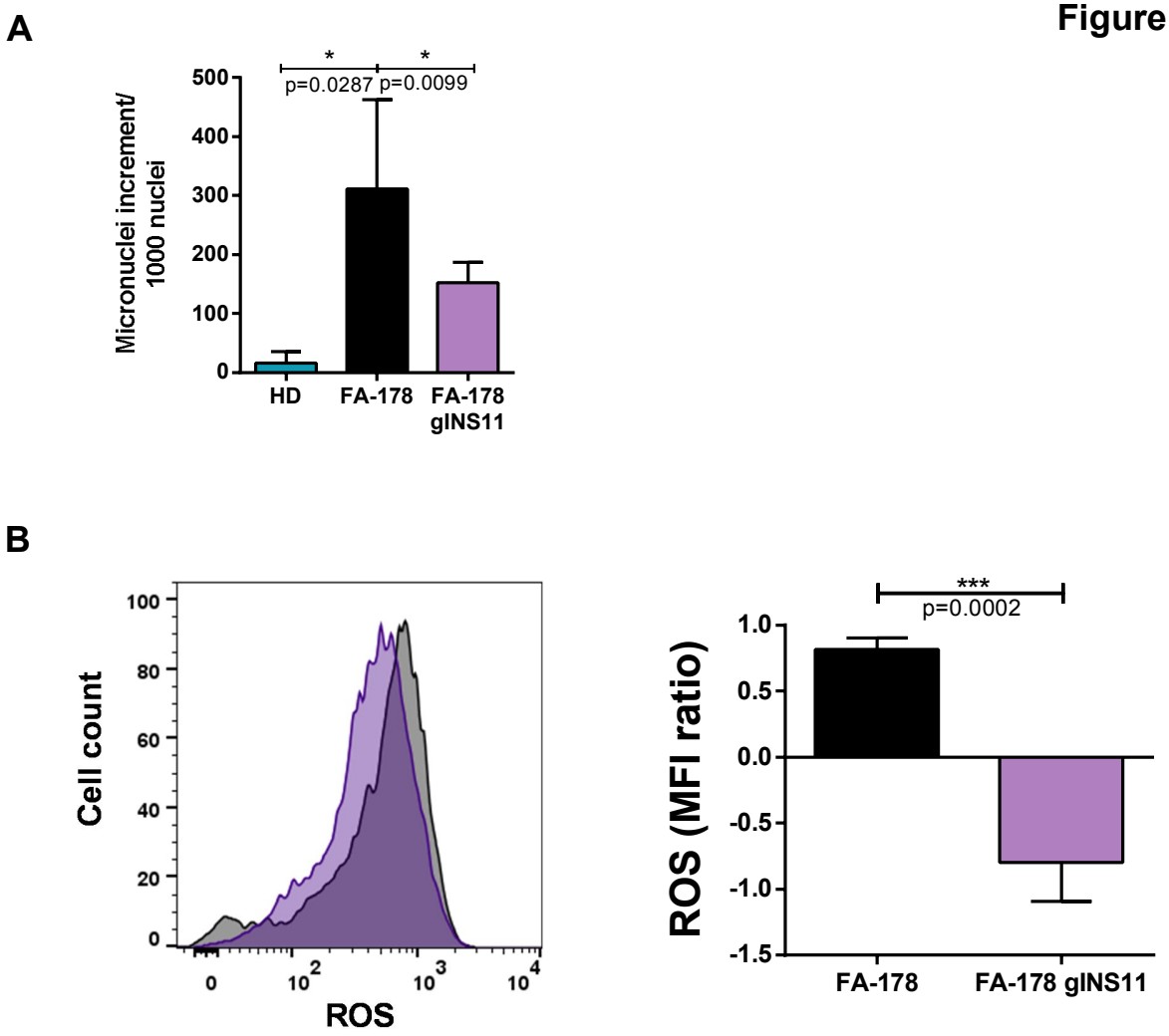

Figure S2. Fanconi anemia phenotypic correction in edited FA-178 LCLs, Related to Figure 1. (A) Chromosomal fragility measured by the reduction in the number of micronuclei in edited FA-178 LCL (purple) when exposed to DEB in comparison to untreated FA-178 LCL (black). Bars represent mean ± SD of three different analyses. An unpaired t-test was conducted. (B) Edited FA-178 LCL showed a reduction in ROS production. ROS production was measured in FA-178 LCL after NHEJ-mediated editing (purple) and compared with untreated FA-178 control LCL (black). Left panel: ROS mean fluorescence intensity (MFI) representative histogram. Right panel: decrease in ROS production calculated as the MFI ratio of ROS in edited cells compared to untreated ones. Bars represent mean ± SD of three different analyses. An unpaired t-test was conducted.

Figure S3

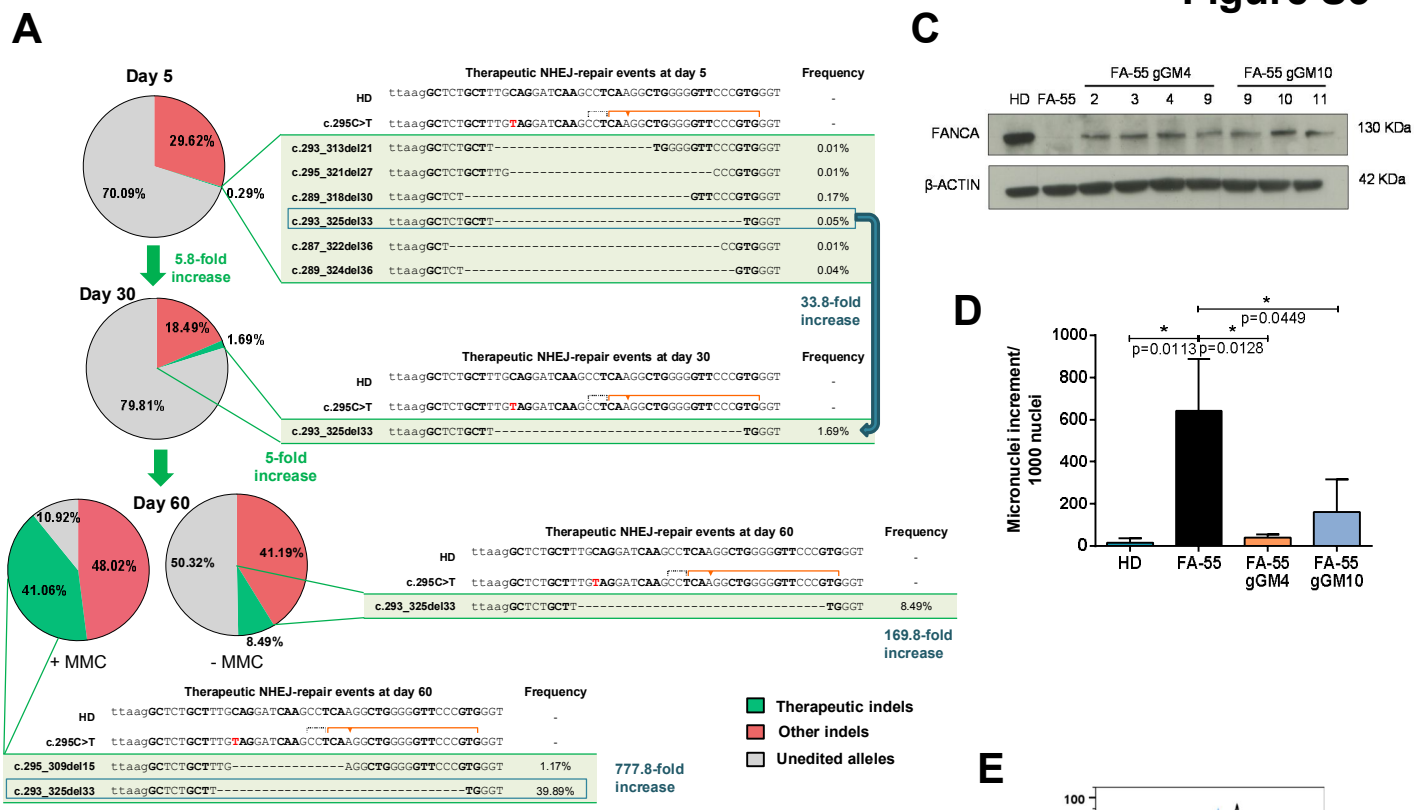

B

LCL	Clone	Allele	Editing	Sequence
FA-55 gGM4	2	1	c.295_309del15	ttaagGCTCTGCTTTG----------AGGCTGGGGGTTCCCGTGGGT
		2	c.300_320del21	ttaagGCTCTGCTTTGTAGGA----------TCCCGTGGGT
	3	1	c.295_309del15	ttaagGCTCTGCTTTG----------AGGCTGGGGGTTCCCGTGGGT
		2	c.300_320del21	ttaagGCTCTGCTTTGTAGGA----------TCCCGTGGGT
	4	1	c.295_309del15	ttaagGCTCTGCTTTG----------AGGCTGGGGGTTCCCGTGGGT
		2	c.300_320del21	ttaagGCTCTGCTTTGTAGGA----------TCCCGTGGGT
	9	1	c.293_325del33	ttaagGCTCTGCTT----------TGGGT
		2	c.311delG	ttaagGCTCTGCTTTGTAGGATCAAGCCTCAA-GCTGGGGGTTCCCGTGGGT
FA-55 gGM10	9	1	c.289_318del30	ttaagGCTCT----------GTTCCCGTGGGT
		2	c.304_311del8	ttaagGCTCTGCTTTGTAGGATCAA--------GCTGGGGGTTCCCGTGGGT
	10	1	c.289_318del30	ttaagGCTCT----------GTTCCCGTGGGT
		2	c.304_311del8	ttaagGCTCTGCTTTGTAGGATCAA--------GCTGGGGGTTCCCGTGGGT
	11	1	c.289_318del30	ttaagGCTCT----------GTTCCCGTGGGT
		2	c.304_311del8	ttaagGCTCTGCTTTGTAGGATCAA--------GCTGGGGGTTCCCGTGGGT

F

Therapeutic NHEJ-repair events at day 5 — Frequency

HD ttttgtgtttaagGCTCTGCTTTGCAGGATCAAGCCTCAAGGCTGGGGGTTC -
c.295C>T ttttgtgtttaagGCTCTGCTTTGTAGGATCAAGCCTCAAGGCTGGGGGTTC -

c.285_305del21	ttttgtgtttaagG----------CTCAAGGCTGGGGGTTC	1.53%
c.289_303del15	ttttgtgtttaagGCTCT----------GCCTCAAGGCTGGGGGTTC	0.9%
c.293_298del6	ttttgtgtttaagGCTCTGCTT------ATCAAGCCTCAAGGCTGGGGGTTC	0.73%
c.292_306del15	ttttgtgtttaagGCTCTGCT----------TCAAGGCTGGGGGTTC	0.45%
c.293_302del9	ttttgtgtttaagGCTCTGCTT---------AAGCCTCAAGGCTGGGGGTTC	0.27%
c.291_299del9	ttttgtgtttaagGCTCTGC---------TCAAGCCTCAAGGCTGGGGGTTC	0.24%
c.293_304del12	ttttgtgtttaagGCTCTGCTT----------CCTCAAGGCTGGGGGTTC	0.08%
c.291_302del12	ttttgtgtttaagGCTCTGC----------AGCCTCAAGGCTGGGGGTTC	0.06%

G

Therapeutic NHEJ-repair events after MMC treatment — Frequency

HD ttttgtgtttaagGCTCTGCTTTGCAGGATCAAGCCTCAAGGCTGGGGGTTC -
c.295C>T ttttgtgtttaagGCTCTGCTTTGTAGGATCAAGCCTCAAGGCTGGGGGTTC -

c.289_303del15	ttttgtgtttaagGCTCT----------GCCTCAAGGCTGGGGGTTC	18.77%
c.285_305del21	ttttgtgtttaagG----------CTCAAGGCTGGGGGTTC	12.08%
c.288_302del15	ttttgtgtttaagGCTC----------AGCCTCAAGGCTGGGGGTTC	5.27%
c.292_306del15	ttttgtgtttaagGCTCTGCT----------TCAAGGCTGGGGGTTC	4.46%
285_296del12	ttttgtgtttaagG----------GGATCAAGCCTCAAGGCTGGGGGTTC	3.38%
c.293_298del6	ttttgtgtttaagGCTCTGCTT------ATCAAGCCTCAAGGCTGGGGGTTC	2.31%
c.291_299del9	ttttgtgtttaagGCTCTGC---------TCAAGCCTCAAGGCTGGGGGTTC	1.87%
c.291_302del12	ttttgtgtttaagGCTCTGC----------AGCCTCAAGGCTGGGGGTTC	0.59%

Figure S3. Fanconi anemia phenotypic correction in edited FA-55 LCL and improvement of potentially corrective indels by using a more specific MS-RNP (gGM0), Related to Figure 2. (A) Percentage of indels identified by Next Generation Sequencing 5, 30 and 60 days after editing with gGM4 before and after MMC selection. (B) Sanger sequencing of FA-55 edited clones. NHEJ-corrected alleles are marked in green while non-corrected ones are marked in red. (C) FANCA protein expression was restored in isolated edited FA-55 LCL clones. Panel shows FANCA Western-blot in different isolated clones. β-Actin was used as a loading control. (D) Edited FA-55 LCL (orange and light blue) exhibited a decrease in the chromosomal fragility, measured by the number of micronuclei, when exposed to DEB in comparison to untreated FA-55 LCL (black), acquiring levels similar to a HD LCL (dark blue). Bars represent mean ± SD of three different analyses. An unpaired t-test was conducted. (E) Reduced ROS MFI in NHEJ-edited FA-55 LCL. ROS production was measured in FA-55 LCL after NHEJ-mediated editing (blue) and compared with untreated FA-55 control LCL (black). Upper panel: representative histogram of ROS MFI. Lower panel: decrease in ROS production calculated as the MFI ratio of ROS in edited cells compared to untreated ones. Bars represent mean ± SD of three different analyses. An unpaired t-test was conducted. (F) The design of a more specific, chemically modified sgRNA (gGM0) and its use as a ribonucleoprotein (MS-RNP0) increases the correction efficacy. The most frequent potentially corrective NHEJ-repair events at 5 days after electroporation (F) and after MMC treatment (G) and their frequencies are displayed.

The sequences obtained in the NGS were classified as in Figure 1.

Figure S4

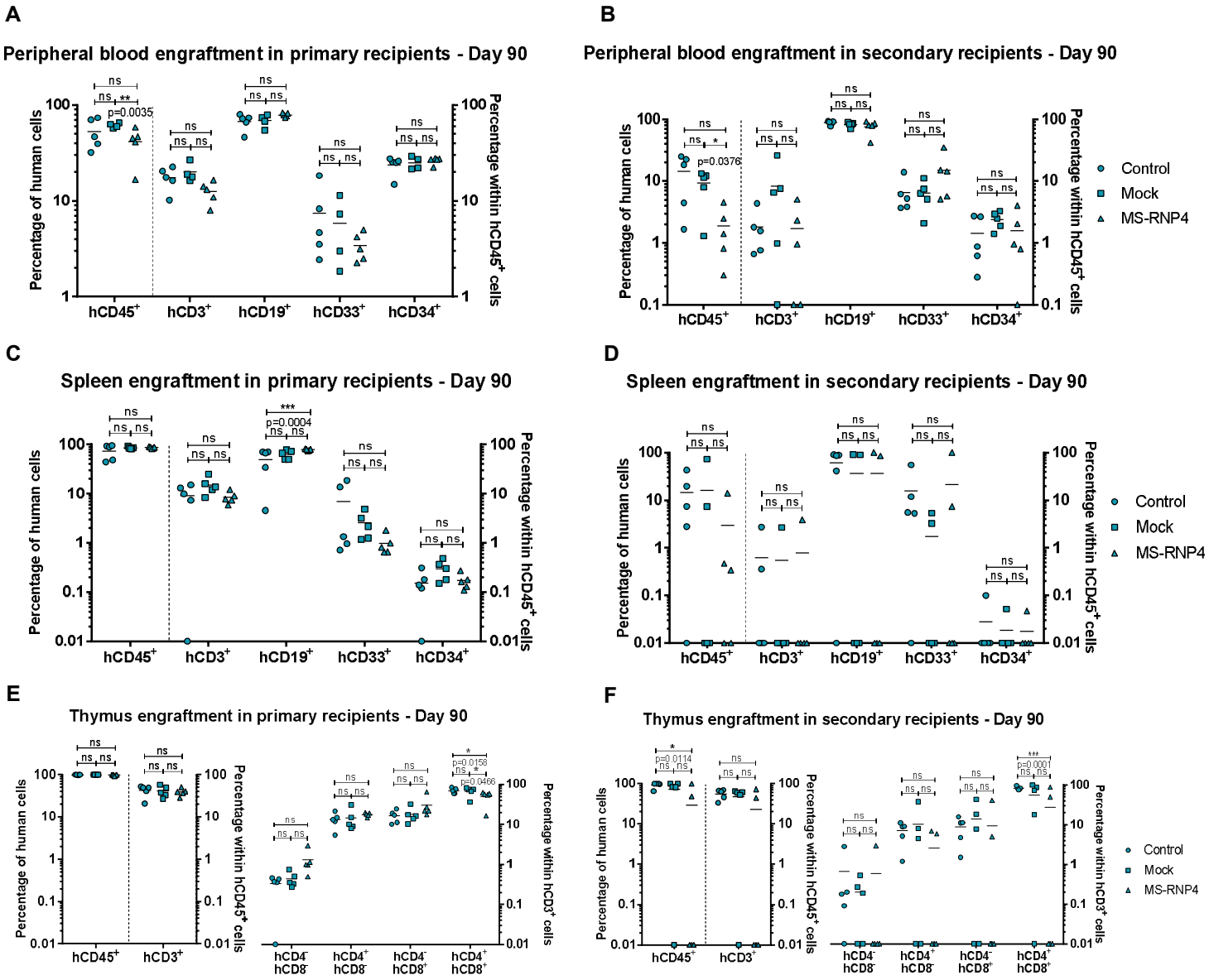

Figure S4. Multi-lineage engraftment of human HSPCs in primary and secondary recipients three months post-transplantation, Related to Figure 4. Peripheral blood reconstitution was evaluated in primary (A) and secondary recipients (B) using antibodies against hCD3 for T cells, hCD19 for B cells, hCD33 for myeloid cells and hCD34 for HSPCs. A two-way ANOVA was performed followed by Tukey's post hoc test in all analyses. Spleen multi-lineage reconstitution was evaluated in primary (C) and secondary recipients (D) using antibodies against hCD3 for T cells, hCD19 for B cells, hCD33 for myeloid cells and hCD34 for HSPCs. Thymus multi-lineage reconstitution was evaluated in primary (E) and secondary recipients (F) using antibodies against hCD3 for T cells. The distinction between cytotoxic and helper T cells was made according to the presence of hCD8 and hCD4 antibodies respectively. Data are represented as mean ± SD.

Figure S5

A

FA-807 BM CD34⁺ CFCs (0 nM MMC)

Allele	Editing	Sequence	Frequency	Phenotype
1	c.288_338del51	ttaag**GC**TC----------A**GCCGG**	3.8% (1/26)	Healthy 50% (13/26)
2	NE	ttaag**GCTCTGCTTTGTAGGATCAAGCCTCAAGGCTGGGGGTTCCCGTGGGTATTCTCTCAGCCGG**		
1	c.289_318del30	ttaag**GCTCT**----------**GTTCCCGTGGGTATTCTCTCAGCCGG**	30.8% (8/26)	
2	NE	ttaag**GCTCTGCTTTGTAGGATCAAGCCTCAAGGCTGGGGGTTCCCGTGGGTATTCTCTCAGCCGG**		
1	c.289_318del30	ttaag**GCTCT**----------**GTTCCCGTGGGTATTCTCTCAGCCGG**	11.5% (3/26)	
2	c.304_311del8	ttaag**GCTCTGCTTTGTAGGATCAA**--------**GCTGGGGGTTCCCGTGGGTATTCTCTCAGCCGG**		
1	c.289_318del30	ttaag**GCTCT**----------**GTTCCCGTGGGTATTCTCTCAGCCGG**	3.8% (1/26)	
2	c.286_320del35	ttaag**GC**----------**TCCCGTGGGTATTCTCTCAGCCGG**		
1	c.304_317del14	ttaag**GCTCTGCTTTGTAGGATCAA**----------**GGTTCCCGTGGGTATTCTCTCAGCCGG**	3.8% (1/26)	FA 50% (13/26)
2	NE	ttaag**GCTCTGCTTTGTAGGATCAAGCCTCAAGGCTGGGGGTTCCCGTGGGTATTCTCTCAGCCGG**		
1	c.311delG	ttaag**GCTCTGCTTTGTAGGATCAAGCCTCAA**-**GCTGGGGGTTCCCGTGGGTATTCTCTCAGCCGG**	7.7% (2/26)	
2	NE	ttaag**GCTCTGCTTTGTAGGATCAAGCCTCAAGGCTGGGGGTTCCCGTGGGTATTCTCTCAGCCGG**		
1	c.310delA	ttaag**GCTCTGCTTTGTAGGATCAAGCCTCA**-**GGCTGGGGGTTCCCGTGGGTATTCTCTCAGCCGG**	3.8% (1/26)	
2	NE	ttaag**GCTCTGCTTTGTAGGATCAAGCCTCAAGGCTGGGGGTTCCCGTGGGTATTCTCTCAGCCGG**		
1	NE	ttaag**GCTCTGCTTTGTAGGATCAAGCCTCAAGGCTGGGGGTTCCCGTGGGTATTCTCTCAGCCGG**	34.6% (9/26)	
2	NE	ttaag**GCTCTGCTTTGTAGGATCAAGCCTCAAGGCTGGGGGTTCCCGTGGGTATTCTCTCAGCCGG**		

B

FA-807 BM CD34⁺ CFCs (3 nM MMC)

Allele	Editing	Sequence	Frequency	Phenotype
1	c.289_318del30	ttaag**GC**TCT----------**GTTCCCGTGGGTATTCTCTCAGCCGG**	14.3% (1/7)	Healthy 85.7% (6/7)
2	NE	ttaag**GCTCTGCTTTGTAGGATCAAGCCTCAAGGCTGGGGGTTCCCGTGGGTATTCTCTCAGCCGG**		
1	c.289_318del30	ttaag**GCTCT**----------**GTTCCCGTGGGTATTCTCTCAGCCGG**	42.9% (3/7)	
2	c.304_311del8	ttaag**GCTCTGCTTTGTAGGATCAA**--------**GCTGGGGGTTCCCGTGGGTATTCTCTCAGCCGG**		
1	c.289_318del30	ttaag**GCTCT**----------**GTTCCCGTGGGTATTCTCTCAGCCGG**	14.3% (1/7)	
2	c.311delG	ttaag**GCTCTGCTTTGTAGGATCAAGCCTCAA**-**GCTGGGGGTTCCCGTGGGTATTCTCTCAGCCGG**		
1	c.289_318del30	ttaag**GCTCT**----------**GTTCCCGTGGGTATTCTCTCAGCCGG**	14.3% (1/7)	
2	c.310_311del2	ttaag**GCTCTGCTTTGTAGGATCAAGCCTCA**--**GCTGGGGGTTCCCGTGGGTATTCTCTCAGCCGG**		
1	NE	ttaag**GCTCTGCTTTGTAGGATCAAGCCTCAAGGCTGGGGGTTCCCGTGGGTATTCTCTCAGCCGG**	14.3% (1/7)	FA 14.3% (1/7)
2	NE	ttaag**GCTCTGCTTTGTAGGATCAAGCCTCAAGGCTGGGGGTTCCCGTGGGTATTCTCTCAGCCGG**		

C

FA-807 BM CD34⁺ CFCs (10 nM MMC)

Allele	Editing	Sequence	Frequency	Phenotype
1	c.289_318del30	ttaag**GC**TCT----------**GTTCCCGTGGGTATTCTCTCAGCCGG**	33.3% (2/6)	Healthy 100% (6/6)
2	NE	ttaag**GCTCTGCTTTGTAGGATCAAGCCTCAAGGCTGGGGGTTCCCGTGGGTATTCTCTCAGCCGG**		
1	c.289_318del30	ttaag**GCTCT**----------**GTTCCCGTGGGTATTCTCTCAGCCGG**	33.3% (2/6)	
2	c.304_311del8	ttaag**GCTCTGCTTTGTAGGATCAA**--------**GCTGGGGGTTCCCGTGGGTATTCTCTCAGCCGG**		
1	c.289_318del30	ttaag**GCTCT**----------**GTTCCCGTGGGTATTCTCTCAGCCGG**	16.7% (1/6)	
2	c.311delG	ttaag**GCTCTGCTTTGTAGGATCAAGCCTCAA**-**GCTGGGGGTTCCCGTGGGTATTCTCTCAGCCGG**		
1	c.289_318del30	ttaag**GCTCT**----------**GTTCCCGTGGGTATTCTCTCAGCCGG**	16.7% (1/6)	
2	c.302_321del20	ttaag**GCTCTGCTTTGCAGGATC**----------**CCCGTGGGTATTCTCTCAGCCGG**		

Figure S5. Sanger sequencing of the *FANCA* exon 4 targeted locus in BM FA-807 hematopoietic CFCs, Related to Figure 6A. The frequency and phenotype of the different allele combination detected in the CFCs are indicated. (A) Colonies obtained in the absence of MMC. (B) Colonies obtained at 3 nM MMC. (C) Colonies obtained at 10 nM MMC. NE = not edited. The c.295C>T mutation is signalled in red. Corrective NHEJ-repair events are marked in green while non-corrective ones are shown in red. Codons are represented by alternating bold and normal upper-case letters and intronic sequence is shown in lower-case letters. The symbol "-" stands for deletion.

Figure S6

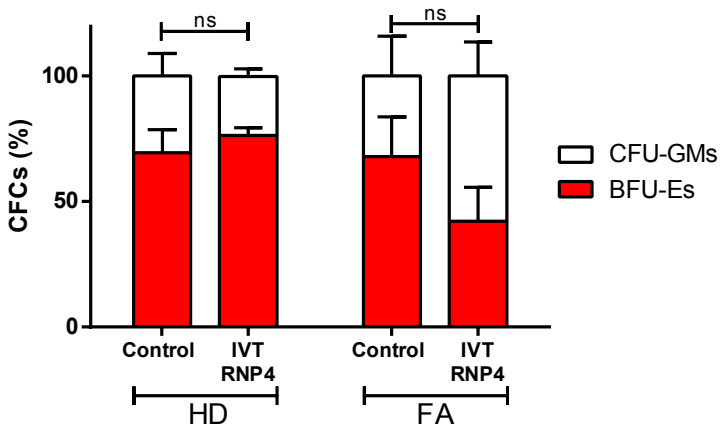

Figure S6. *In vitro* differentiation capacity of edited FA HSPCs, Related to Figures 4, 5 and 6. Similar percentage of erythroid (BFU-Es) and myeloid (CFU-GMs) progenitors were observed *in vitro* in edited FA-HSPCs (N=4) versus unedited or HD cells (N=6). Bars represent mean ± SD. A two-way ANOVA was performed followed by Tukey's post hoc test.

Figure S7

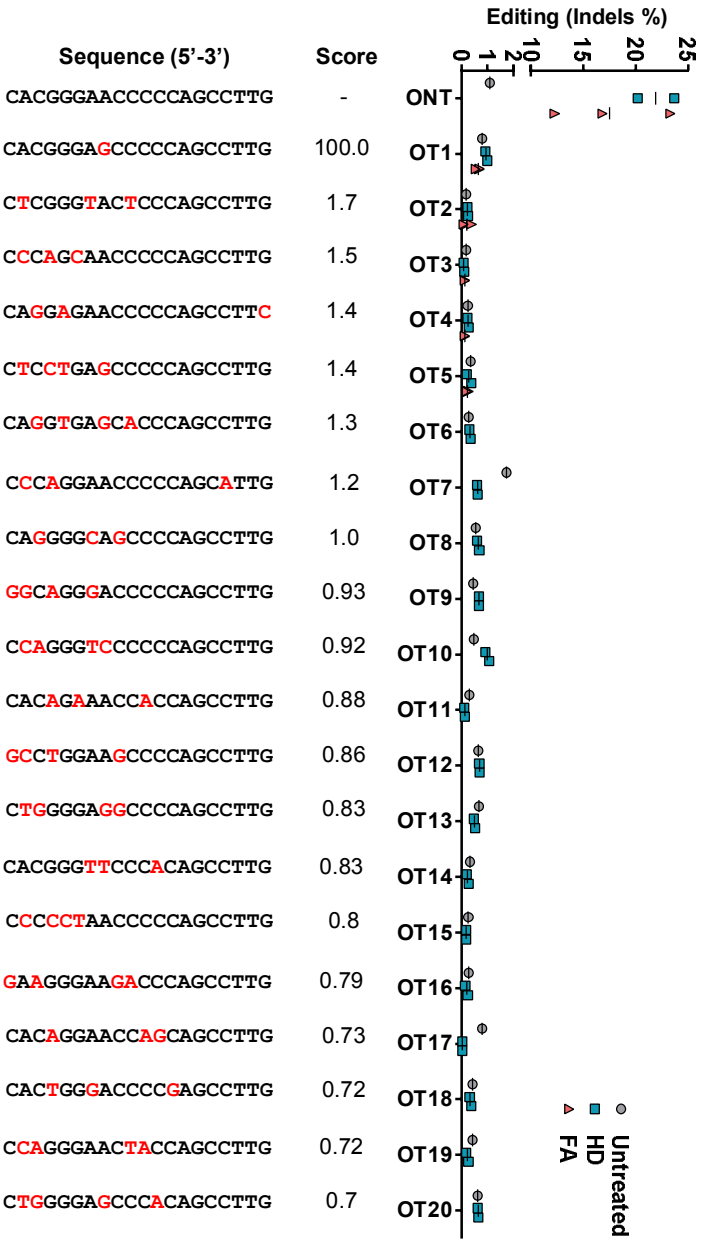

Figure S7. NGS analysis of the top-20 *in silico* predicted off-target loci for gGM4, Related to Figures 4, 6 and 7. The top-5 loci were analysed by NGS in three different samples from FA-A patients bearing the c.295C>T mutation (red triangles) after NHEJ-mediated gene editing using the IVT-RNP4. The top-20 loci were analysed in two edited hCD34^{+} cell samples from healthy donors after editing using IVT-RNP4 (blue squares). Unedited hCD34^{+} cells from a healthy donor were also sequenced control (grey circle). The probability score calculated by the *CRISPR Design Tool* is shown. The mismatches are signalled in red.